Regional-scale probabilistic shoreline evolution modelling for flood-risk assessment

Regional-scale probabilistic shoreline evolution modelling for flood-risk assessment

Stuart Stripling[a1], Michael Panzeri[b], Belen Blanco[c], Kate Rossington[d], Paul Sayers[e], and Alistair Borthwick[f]

[a] School of Engineering, Plymouth University, Drake Circus, Plymouth, PL4 8AA, UK.

stuart.stripling@plymouth.ac.uk

[b]HR Wallingford Ltd., Howbery Park, Wallingford, Oxon, OX10 8 BA, UK

mcp@hrwallingford.com

[c]HR Wallingford Ltd., Howbery Park, Wallingford, Oxon, OX10 8 BA, UK

blb@hrwallingford.com

[d]HR Wallingford Ltd., Howbery Park, Wallingford, Oxon, OX10 8 BA, UK

kro@hrwallingford.com

[e]Sayers and Partners LLP, 24a High Street, Watlington, OX49 5PY, UK.

paul.sayers@sayersandpartners.co.uk

[f]School of Engineering, University of Edinburgh, King's Buildings, Edinburgh, EH9 3JL, UK

alistair.borthwick@ed.ac.uk

Abstract

Rapid deterministic modelling of shoreline evolution at regional and coastal-scheme scale enables Monte-Carlo simulations by which long-term shoreline statistics can be estimated. This paper describes UnaLinea, a fast, accurate finite difference solver of

[1] Corresponding author

the one-line sediment continuity equation. The model is verified for the evolution of an initially straight shoreline of a plane beach subject to regular breaking waves at constant angle of incidence in the presence of either a groyne or a continuous single-point feed of sediment. Grid convergence and stability tests are used to obtain accurate, stable results, with satisfactory computational efficiency. Influences of wave input filtering and event-based sediment loading are considered. The rapid deterministic model is applied to Monte-Carlo simulations of the evolution of the west coast of Calabria, Italy for different scenarios including increased sediment load from a river and selected beach nourishment. The potential role of probabilistic shoreline evolution in regional coastal flood-risk assessment is explored through application to an idealised stretch of the Holderness coastline, U.K., where flood depths and expected damage are estimated for a 1000 year return period event.

Keywords: Shoreline evolution; Flood/Erosion-risk; Probabilistic modelling; Wave filtering; Regional scale

1 Introduction

Beach plan-shape models are widely used in coastal engineering practice. Of these, perhaps the most popular is the one-line model derived from the mass balance of sediment in an elemental volume oriented so that its x-direction width lies in a direction approximately parallel to the shoreline, and its y-direction sides extend offshore up to the closure depth D_c. The model is called one-line because the beach morphology is represented by a single shoreline contour. Changes in position of this contour, together with other parameters such as wave conditions, currents, and sediment transport rates, are functions of longshore position (x) and time (t), and so the model is essentially one-dimensional in space. In the one-line model, it is assumed that the beach profile extending offshore remains constant with time. Bakker *et al.* (1970) provide a very useful starting point for those interested in the theory and application of beach plan-shape models. They discuss the simplest one-line approach and consider profile variation along the shoreline. Horikawa (1988), Komar (1998), Dean and Dalrymple (2002) and Reeve *et al*. (2004) provide derivations of the one-line equation and give examples of its application in practice.

For small angles of wave attack, the one-line equation can be approximated by the (small angle) one-line diffusion beach response equation, originally derived by Pelnard-Considère (1956) for small amplitude departures from a rectilinear coastline (Falqués, 2003). Analytical solutions of the Pelnard-Considère one-line diffusion equation are listed by Le Méhauté and Soldate (1977), Walton and Chiu (1979), Larson *et al*. (1987), Dean and Dalrymple (2002), Falqués (2003), Murray and Ashton (2003), Reeve *et al*. (2004), and Reeve (2006). In practice, most one-line modelling for coastal erosion management is performed using numerical models (see e.g. Hanson and Kraus, 1989; Ozasa and Brampton, 1980), due to their flexibility in

modelling realistic, non-idealised coastlines that include seawalls and complicated groyne systems.

Although one-line models have been used to inform coastal management decisions for about 40 years, the use of multi-realisation simulations for probabilistic purposes is a recent development, and to date relatively little attention has been paid to their application to the generation of long-term beach response statistics (Wang and Reeve, 2010). To achieve multiple realisations for probabilistic analysis, a numerical one-line model must be accurate, reliable, and computationally efficient. Such a model requires the solver to be simple yet appropriate, and that the grid spacing and time step be as large as possible while retaining accuracy and stability. Finite-difference schemes are commonly used to solve the one-line equation. Second- and higher-order explicit numerical schemes are conditionally stable in that they have a limited region of stability in terms of the time step and grid spacing (see e.g. Fletcher, 1990). Implicit schemes are (theoretically) unconditionally stable thus allowing much larger time-steps to be used, but are more complicated to code and can be more computationally intensive. In practice, the time-step of an implicit scheme is restricted due to the presence of numerical round-off errors (Zacharioudaki and Reeve, 2010). One-line models are particularly prone to instability when applied to cases involving complicated infrastructure layouts and/or requiring large grids at regional scale. Although instability can be managed through intervention by a modeller undertaking a single deterministic application, this is not feasible in a probabilistic application where many thousands of individual deterministic runs may have to be realised.

This paper extends one-line modelling to probabilistic application through the use of a computationally-efficient one-line numerical model, named UnaLinea.

UnaLinea has been developed with the specific intent to produce multiple, regional-scale, and long-term simulations for the probabilistic assessment of shorelines where event-based processes, such as cliff falls, artificial nourishment or fluvial loading, and their influence on coastal evolution, can be rapidly predicted. It is also demonstrated how the probabilistic application can be used to enhance the assessment of coastal flood-risk over a timescale of decades at regional scale. The structure of the paper is as follows. Section 2 describes the one-line equation and the UnaLinea numerical solver. Section 3 presents model convergence and verification test results against analytical solutions. Section 4 discusses filtering of the wave input to permit longer time-steps to be utilised, introducing the concept of "morphologically-averaged conditions". Section 5 considers regional-scale application, while Section 6 presents a demonstration case of Monte-Carlo simulation using the UnaLinea model. Section 7 describes a further application of the UnaLinea model with the RASP Structured Uncertainty (RASP-SU) flood risk model (Gouldby *et al*. 2010) within a GIS framework. The main conclusions are summarised in Section 8.

2 UnaLinea one-line model development

The one-line equation expresses volumetric conservation of sediment moving along the shoreline as follows (see e.g. Dean and Dalrymple (2002)),

$$\frac{\partial Q}{\partial x} + \frac{\partial A}{\partial t} + q_c = 0 \qquad (1)$$

where Q is the volumetric rate of alongshore sediment transport, x is the distance along the shore, A is the beach cross-sectional area, t is time, and q_c is the volume flux of material in the cross-shore direction expressed as a line source. Denoting the co-ordinate perpendicular to the beach by y, the beach cross-sectional area, A, can then be expressed as the product of y and a depth D. If D (the depth of the active profile,

defined by the summation of the closure depth and the berm height) is assumed not to vary with time, then equation (1) can be written

$$\frac{\partial Q}{\partial x} + D\frac{\partial y}{\partial t} + q_c = 0 \qquad (2)$$

Starting from some initial position, $y = y(x)$, the model evaluates successive beach positions at time intervals Δt, at points along the shore separated by Δx. So for each ordinate x_i (separated from its neighbour x_{i+1} by Δx) the beach position is given by $y_i(n\Delta t)$ for $n = 0, 1, 2 \ldots$ at $t = n\,\Delta t$. The beach position occupies a single contour, which normally represents the high water line.

An important factor regarding model accuracy is the representation of the alongshore rate of sediment transport, Q, which is dominated by the action of breaking waves. For waves of small unevenness in height along a beach with nearly straight contours, Q is approximated by the CERC (1984) formula. Incorporating the Osaza and Brampton (1980) term for alongshore variation in wave height, Q is given by:

$$Q = H_{sb}^2 C_g \left(AK_1 \sin 2\alpha_b - \frac{B}{\tan\beta} K_2 \cos\alpha_b \frac{dH_{sb}}{dx} \right) \qquad (3)$$

where A and B are non-dimensional parameters, α_b is breaking wave angle, H_{sb} is significant wave height at breaking, C_g is group celerity, K_1 and K_2 are sediment transport coefficients, and β is beach slope.

Expanding equation (2) by substitution of Q from equation (3) reveals that the one-line equation is an advection-diffusion equation, which is dominated by diffusion provided the wave angle is less than 45 degrees. In Unalinea, equation (2) is solved numerically using central differences in space and a first-order accurate forward Euler explicit scheme in time. For the small-angle approximate one-line model, where

$\frac{\partial y}{\partial t} = \frac{2Q_0}{D}\frac{\partial^2 y}{\partial x^2}$ (see e.g. Larson *et al*. 1987) where Q_0 is the amplitude of the longshore sand transport rate, then a forward-time centred-space scheme would be (theoretically) stable provided $\Delta t \leq \frac{D\Delta x^2}{4Q_0}$. This agrees with the approach taken by Krauss and Harikai (1983). This criterion indicates that a doubling of the grid spacing should allow a four-fold increase in Δt. However, noting that the full one-line equation comprises advection, diffusion and possibly source-terms, it is difficult to evaluate a catch-all stability criterion *a priori*, and so we resort herein to numerical experiments (following advice from e.g. Roache, 1998).

3 One-line probabilistic modelling at regional scale

3.1 Case AS1 – single groyne

Case AS1 concerns the impact of an infinitely long impermeable groyne inserted at the middle of an initially plane beach subject to regular waves of height 1.5 m, period 6 s, at a fixed angle of incidence of 10º. The offshore depth at which waves are input is 12 m, the mean grain size of the sediment D_{50} is 0.00099 m, the coefficient K_1 is 0.1687, the depth of active beach is 6 m, and the simulation epoch is 2 months. For a detailed coastal design study, the grid spacing Δx would be of the order of 10 m to resolve precisely the shoreline evolution in the vicinity of the groyne. However, to achieve a rapid probabilistic 1-line model able to cover regional scales, where detailed design is not necessary, larger grid-sizes may be used to achieve high computational performance whilst ensuring that the solutions are satisfactorily accurate. A grid convergence test was undertaken using a range of grid spacing including Δx = 100, 200, 250, and 400 m. Satisfactory results were obtained for all grid-sizes, though

discrepancies became noticeable for Δx > 250 m. In this case, Δx = 200 m appears appropriate for one-line modelling at regional-scale. In practice, care should be taken to carry out further grid convergence checks to ensure that a converged estimate is achieved of maximum shoreline recession and flood risk parameters. Figure 1 shows the numerical (UnaLinea) and analytical shoreline (AS) profiles obtained after 1 month and 2 months, using the converged grid with a time step of 1 day. Note that maximum and minimum shoreline positions appear to diminish with increasing grid-spacing, a shortcoming that can be overcome, if required, by extrapolation.

FIGURE 1

We now turn to stability. For a detailed design study, hourly or 3-hourly wave conditions would typically be input in a deterministic one-line model. Much larger time-steps are desirable in a rapid probabilistic one-line model at regional scale. Figure 2 shows the model predictions obtained for time steps varying from Δt = day to month, compared against the analytical solution. Satisfactory predictions are achieved for Δt = week, but divergence from the analytical solution through instability is noticeable from Δt = fortnight and apparent throughout the model domain for Δt = month.

FIGURE 2

3.2 Case AS2 – event-based point source

Case AS2 examined the evolution of an initially straight shoreline at a plane sloping beach when a constant supply of sediment was added as a single point source. This is

considered representative of, for example, river-loading, a beach recharge programme, or a series of cliff-falls. The point source was located in the middle of the model domain (0.0 m), of the same order of magnitude as the initial longshore drift rate, and again subject to regular waves of low angle of incidence. The same input parameters were used as in Case AS1, and tests undertaken for grid convergence, stability, and choice of solver. The grid convergence tests were undertaken for Δx = 75, 100, 150, 200, 250, 300, and 400 m, with satisfactory results achieved for Δx < 300 m. Figure 3 shows model predictions of the evolved shoreline after one and two months. Although the initial longshore drift rate is of the same order of magnitude as the point source, the drift rate reduces due to wave refraction. Here, the planform evolution is dominated by the diffusive and the point source terms, and is marginally asymmetric. For Δx = 250 m and Δt = 1 day; the predictions are in excellent agreement with the analytical solutions.

FIGURE 3

Figure 4 presents the results obtained when varying the time-step, indicating that Δt = 1 week provides an appropriate balance between computational speed and stability.

FIGURE 4

3.3 Grid-convergence, stability and choice of numerical solver

From the foregoing tests, it may be concluded that Δx ~ 200 m and Δt ~ 1 week are appropriate for both the groyne (Case AS1) and the point source (Case AS2) considered here. Table 1 compares the stability ranges obtained for Case AS1 and

Case AS2, highlighting the need to identify suitable values for Δx and Δt before carrying out multiple long-term probabilistic simulations at regional scale.

TABLE 1

4 Filtering of wave input

In probabilistic modelling, it often takes several weeks of computer processing before outcomes can be realised. Wave-filtering represents a powerful technique that enables very large increase in time-step with consequent reduction in computer run time. Here, the wave climate time-series is reduced to a series of sequential "morphologically-averaged" conditions. "Morphologically-averaged" conditions, which may be daily or weekly forcing conditions expressed as wave height, period, and direction, are those that induce the equivalent amount of net longshore drift as for the same length of hourly or 3-hourly records. A typical application might be to reduce a 20-year wave time-series at 3-hour intervals (~3000 conditions per annum) to 20 years of morphologically-averaged conditions derived at weekly intervals (~50 conditions per annum); in such circumstances, the forcing conditions would change, but the total amount of sediment moved throughout the year would effectively be the same. Wave filtering, along with optimised grid spacing and time-step, could be expected to allow probabilistic outcomes to be obtained within minutes say, on a present-day PC.

The principles behind wave filtering are applied to a scatter diagram where wave height is classified against wave direction, with each wave height bin (H_i) and each wave direction bin (θ_j) within the scatter diagram having a certain number of

occurrences (n_{ij}). The total number of occurrences in the scatter diagram is given by N so that $\sum n_{ij} = N$.

The potential longshore sediment transport for each wave condition (H_i, θ_j) can be estimated by the CERC formula (given in the first part of equation 3) as:

$$q_{ij} = \frac{n_{ij} H_i^{2.5} \sin 2(\theta_j - \Phi)}{N} \quad (4)$$

where Φ is the angle of the beach normal and n_{ij}/N represents the relative frequency of occurrence. In this estimate, the effect of the wave period through the wave celerity is included via the shallow-water approximation. The sum of all of the potential longshore drifts within the scatter diagram, Q_{tot}, is then given by:

$$Q_{tot} = \sum q_{ij} \quad (5)$$

We wish to find a condition that represents the wave climate in terms of longshore drift for a given beach orientation. That representative condition (H, θ) is derived from the following definitions:

1) The "neutral" shoreline orientation, θ, that would render the offshore wave climate producing a zero net drift:

$$\sum n_{ij} H_i^{2.5} \sin 2(\theta_j - \theta) = 0 \quad (6)$$

and

2) The representative wave height, H, that would produce, together with the representative angle, θ, the same drift (Q_{tot}) as all the conditions it is representing:

$$H^{2.5} \sin 2(\theta - \Phi) = Q_{tot} \quad (7)$$

Starting with the formula for the sine of subtracted angles, trigonometry allows equation 6 to be expressed as:

$$\sum n_{ij} H_i^{2.5} \left[\sin 2\theta_j \cos 2\theta - \cos 2\theta_j \sin 2\theta \right] = 0 \qquad (8)$$

which, again using trigonometry, becomes:

$$\tan 2\theta = \frac{\sum n_{ij} H_i^{2.5} \sin 2\theta_j}{\sum n_{ij} H_i^{2.5} \cos 2\theta_j} \qquad (9)$$

Equation 9 can be solved to obtain the representative wave direction θ.

Substituting equation 5 in equation 7 we can obtain a solvable expression for the representative wave height, H:

$$H^{2.5} = \frac{\sum n_{ij} H_i^{2.5} \cos 2\theta_j}{N \cos 2\theta} \qquad (10)$$

Two of the four possible values for θ lead to $H^{2.5}$ being negative (and therefore H being complex) and so are rejected. Two possibilities for H and θ remain, differing only in θ by 180º; in almost all cases, only one of these is physically sensible. The time-series data also contain the wave period associated with (H_i, θ_j) at each time-step, and so the representative wave period is determined as the mean of these values. Time-series data with zeros for values of wave height or wave period are treated as calm. The wave-filtering method ignores calm data in evaluating the morphologically-averaged wave conditions. The total calm period is determined by summation, from which the proportion of time is calculated for which there are no calm data. This proportion is used as a multiplier of the longshore drift during that time step to account for calm periods. Representative forcing conditions are derived from those driving the longshore transport calculations (i.e. at the wave breaking

point) by backwards refraction offshore until reaching the depth associated with the original time-series.

The wave-filtering approach has the limitation that subtle changes to the direction of transport of sediment in the short term may be missed; this limitation is considered when selecting the timeframe over which the morphologically-averaged condition is derived. Furthermore, the morphologically-averaged condition is based on estimated longshore drift rates, and calibration of UnaLinea would be required to increase confidence in model outcomes,

5 Regional considerations

Regional applications often involve a range of backshore features, such as seawalls and soft-cliffs. UnaLinea incorporates certain measures to accommodate the effect of such features, including allowance for seasonal variations on the beach profile, and a soft-cliff recession model.

5.1 Accommodating seasonal beach profile changes

Many beaches have seasonally-varying characteristics. The beach slope may flatten during the winter, effectively pivoting around a point (below mean sea level) on the profile, resulting in a landward transition of the mean high water mark and an associated reduction in beach width. The winter climate may be more energetic than the summer, and so there is an increased likelihood of cliff-failure or over-topping of seawalls. To capture this seasonal beach behaviour, if relevant, UnaLinea can be operated with typical summer and winter beach slope values. Figure 5 shows this schematically, where *ypos* is the position of the tracked contour relative to the model baseline. Summer and winter swash limits are denoted by *Yswash_summer* and

Yswash_winter; their variation potentially lowers the defence standard of the beach, here fronting a cliff with cliff-top position (*cpos*) and slope (*cslope*).

FIGURE 5

5.2 Simple cliff-recession model

The simplified cliff-recession model within UnaLinea is computationally fast and gives plausible results. The model relies on expert judgement, permitting minimal representation of the physics of soft-cliff recession. In practice, the user must seek expert advice on calibration to ensure that the cliff-recession model operates within acceptable bounds. The present model divides the regional stretch of shoreline into Cliff Behavioural Units (CBUs) for which the general process of cliff steepening, failure, and re-stabilising is established (Lee and Clark 2002, Ohl *et al*. 2003).

Figure 6 shows a schematic view of the landward migration of the cliff-top caused by beach recession. Whilst there is adequate beach width (yswash>ctoepos) in front of the cliff to protect against erosion, the cliff is considered to be stable (Figure 6a). If the beach width reduces in front of the cliff (ypos and yswash recede), such that the beach berm is eroded, any further recession of the beach will steepen the cliff slope (cslope) – increasing its propensity to fail (Figure 6b). During this process, *Volume*1 of cliff material is added to the beach. Within a CBU, the cliff can be expected to fail when its slope reaches an average angle α_f, and will, after failure, adopt an angle α_s. Since neither α_f nor α_s can be predicted precisely, the model compares the cliff slope against a range of values for which the cliff would become unstable. This range is CBU-dependent, requires expert judgement, and a linear probability distribution of cliff failure is assigned, between 0 at the lower slope and 1

at the higher slope. A random number is generated by the cliff module, and if this is less than the probability of cliff failure, the cliff fails. If the cliff is deemed to fail (Figure 6c), the stable post-failure slope α_s is selected randomly within a range established for the CBU. The cliff top retreats and *Volume*2 of sediment is released on to the beach.

FIGURE 6

The model input comprises the cliff height, toe position, cliff-top position, and information from a geomorphological assessment of pre- and post-landslide angles. The shoreline evolution model determines the time-history of the toe-position, which is useful in assessing the protection afforded to the base of the cliff by the beach (allowing also for seasonal variations). To account for possible variations in α_f and α_s, and the controlling influence of beach width (which is dependent on the order of morphological events) on cliff-toe recession, UnaLinea is run in probabilistic mode when coupled with the cliff-recession module. UnaLinea does not permit cliff-toe recession along shoreline lengths protected by seawalls. If the berm is lost, then the beach level is drawn down at the defence line. The elevation of the beach at the toe of the defence structure (or 'toe level') is recorded at yearly intervals. Through multiple realisations of the probabilistic model, an annual histogram of toe levels is produced for each model node that is backed by seawalls or flood defences.

6 Probabilistic simulation: Fiume Savuto Case Study

Probabilistic shoreline model applications include evaluations of event-based occurrences such as cliff-falls, river loadings, beach nourishment/ mining events, and

beach recycling, based on probability distributions of sediment loadings. Stochastic modelling of shoreline evolution at regional scale has hardly been reported to date in the literature; an exception is the probabilistic application of a one-line model at scheme-scale by Wang and Reeve (2010).

It is not uncommon for 20-years or more of high-resolution time-series of wave conditions to exist at a site of interest. Such extensive datasets are useful for probabilistic modelling. Using the wave-filtering technique described above, it is possible to derive, say, 20 independent years of 52 morphologically-averaged conditions, with each year retaining seasonality. By random sampling these years, it is possible to construct a longer synthetic time-series of forcing conditions likely to occur at the site of interest. UnaLineaProb (the UnaLinea model run in probabilistic mode) provides for multiple simulations based on randomly sampled years of morphologically-averaged events, effectively a synthetic time-series of events which retains seasonality, and event-based loads. Multiple deterministic realisations allow a probabilistic representation of the beach position to be established. At each grid point, therefore, the mean and standard deviation are established of the final beach position (Y_{final}), the average beach position (Y_{avge}), the minimum beach position (Y_{min}), and the maximum beach position over (Y_{max}). Figure 7 presents a flowchart describing the UnaLineaProb algorithm. UnaLineaProb creates a prescribed number of realisations, each of which is assigned a randomly sampled year of morphologically averaged-conditions up to the number of years of interest. This allows long time periods to be examined, and ensures that the seasonality of the time series is preserved. Years are sampled with replacement and the same years are selected for all time-series within the model domain so that dependence between series is not lost. After a certain initial number of realisations, convergence is checked periodically by

monitoring the variance of the total sum of Y_{avge} over all grid points. After each realisation of UnaLinea, values of Y_{final}, Y_{avge}, Y_{min} and Y_{max} over n years are used to update their running means and standard deviations at each grid point. Statistics are also established for other beach parameters, such as toe levels at seawalls.

FIGURE 7

The following case study considers the effect of changes to the fluvial loading of the Fiume Savuto (Figure 8) on the west coast of Calabria, Italy. This case study demonstrates the use of UnaLineaProb in assessing the impact of different event-based sediment loadings on shoreline evolution. The model results presented here should not be treated as absolute (due to limited calibration), but instead are comparative relative to each other. The model study is carried out within the GIS framework reported by Stripling *et al*. (2007) and Stripling and Panzeri (2009).

FIGURE 8

Aggregate extraction from the riverbed of the Fiume Savuto (Plate 1) has caused its bed slope to reduce, so much so that more than one flood event is necessary to enable fluvial sands and gravels to reach the coastline. With much reduced sediment supply to the coastline, coastal erosion and sea defences can now be found in the vicinity of the river mouth (Plate 2).

PLATE 1

PLATE 2

Figure 8 indicates the entire extent of the modelled coastline, the initial position of which was extracted from aerial photographs taken in 2003. Wave conditions at the site were derived from a regional-scale shallow-water wave propagation model (Stripling and Panzeri, 2009) and filtered to provide daily morphologically-averaged conditions. Littoral drift volumes were prescribed to provide a marked response by the coastline, purely for demonstration purposes. Net longshore drift is from north to south .

Figure 9 shows the assumed present distribution of fluvial sediment load expected to arrive at the coastline over a range of flood events. At each time-step, a loading event is sampled based on the daily likelihood of occurrence. Since the Fiume Savuto supplies sediment to the coast only during rare flood events, the majority of the samples return a zero supply volume.

FIGURE 9

Figure 10a presents the shoreline evolution outcomes of two probabilistic simulations each covering 20 years from present: the dotted lines are obtained for no change in fluvial sediment loading from the Fiume Savuto; the solid lines are obtained for a fivefold increase in fluvial sediment loading. Note that neither set of values necessarily occurs concurrently. Indeed, the mean shoreline position after 20 years, and its maximum (furthest seaward) and minimum (furthest landward) positions are derived from the entire set of probabilistic realisations; requiring about 300 realisations before convergence is achieved. It can be seen that the assumed present-

day sediment load distribution from the Fiume Savuto is not sufficient to prevent severe erosion of the coastline downdrift of rigid coastal features. Further, should the river-bed be re-profiled to induce five times the present-day sediment load, there would still be insufficient beach-building material arriving at the coast. The maximum shoreline position suggests that there may be a temporary formation of a delta should sediment loading from the river be increased. The littoral regime, however, is too dynamic for the delta formation to persist.

FIGURE 10

In terms of fluvial and coastal management, artificial nourishment of the eroding downdrift beaches may be an option. Figure 10b presents the likely shoreline behaviour over a 20 year epoch when 40,000 m^3 of nourishment is added annually to the beach immediately south of the river mouth. The dotted lines represent the shoreline response when the nourishment material is introduced monthly throughout the year while the solid lines represent the shoreline response when the nourishment material is added in a single mobilisation every May. Figure 10c shows the effect of adding different volumes of nourishment material, where the dotted and solid lines represent addition each year of 20,000 m^3 and 50,000 m^3 respectively of beach material added in a single mobilisation each year.

Probabilistic modelling supports planning of the timing and location of nourishment. For example, Figure 8 suggests there are two areas downdrift (south) of the Fiume Savuto which could experience significant degrees of erosion. Figure 10b, however, implies that a single nourishment location immediately south of the river would be adequate to manage the tendency of the coastline further downdrift to erode.

This finding corroborates the 'Sandscaping' or 'Sand Engine' approach to shoreline management that is currently the subject of much research (Mulder and Tonnon 2010, Tonnon *et al.* 2014). This case study has illustrated how probabilistic modelling can be applied in coastal management practice.

7 Integrated modelling of erosion-/flood-risk

To provide an integrated regional assessment of erosion and flood risks requires the analysis to be supported by probabilistic methods. One example of an integrated modelling system is the Regional Coastal Simulator (Pearson *et al.* 2005), which originated from a soft-cliff erosion model (Walkden *et al*. 2000). In identifying its potential to expand into the realm of flood-risk assessment, Pearson *et al*. (2005) observed that suitable model linkage was vital. The model output was stored in a GIS database (see e.g. Dawson *et al*. 2005, Bates *et al*. 2005 and Koukoulas *et al*. 2005) allowing wave propagation, morphological, flood-spread and economic damage model results to be queried within the same platform. A second example is the FluidEarth (OpenMI) initiative (eg Fotopoulos *et al*. 2010) which adopts a standard format for the exchange of data between different environmental models. Recognising the ability of GIS to manage large quantities of data, Stripling *et al.* (2007) examined an alternative approach which linked deterministic numerical models of coastal processes within a GIS framework in order to populate the database directly. Stripling and Panzeri (2009) describe the feasibility of such a system supporting assessments of coastal erosion risk and flood risk based on numerical wave propagation, sediment transport, and beach morphology models, empirical parametric models, and data analysis tools. The work reported here builds upon the approach of Stripling and Panzeri (2009) in two ways. First, a relational database is utilized for

efficient, logical storage of all model input, output, calibration and management data rather than in 'flat-files' (Panzeri and Stripling, 2012). Second, the modelling methods are extended to probabilistic applications, where computational efficiency gains are important.

Being regional, UnaLineaProb can incorporate the effects of shoreline defence structures, changes in beach volume caused by cliff-erosion, and changes to sediment supply from rivers. The present paper presents a proof-of-concept application, rather than a calibrated representation, of the integrated erosion-risk and flood-risk models along a 50 km length of shoreline on the east coast of England, Holderness, from Flamborough Head to Spurn Head (Figure 11). As is likely at regional scale, this shoreline is characterised by various features, including sandy beaches backed by eroding cliffs. An urban area, situated where the cliffs heights diminish, is protected by beach and structural defences such as seawalls and groynes.

FIGURE 11

7.1 Enhancement of the RASP-SU modelling method

In England and Wales, the Environment Agency (EA), has used RASP (Risk Assessment for Strategic Planning) approaches (Sayers and Meadowcroft 2005) to undertake national scale assessments of flood risk (NaFRA – National Flood Risk Assessment) on a routine basis since 2002 (Hall *et al*. 2003, Gouldby *et al*. 2008). Comprehensive risk analysis should include consideration of uncertainties (Bedford and Cooke, 2001), and so a version of RASP was developed (McGahey and Sayers 2008) that incorporated aleatory uncertainty associated with random events such as future floods. RASP-SU (HR Wallingford (2009), Gouldby *et al.* 2010) was

developed to consider the forward propagation of epistemic uncertainties associated with lack of knowledge (e.g. defence crest level) from individual input parameters to the final output of overtopping volumes, flood depths and probabilities, and expected annual damage. RASP-SU allows for toe-level uncertainty within the extreme event overtopping calculations making its predictions directly compatible with those of UnaLineaProb when flood defence structures exist along the coast. The two models were coupled together in a GIS framework (Stripling and Panzeri 2007) by establishing spatial connectivity between the UnaLinea model nodes and the sea defences in the RASP-SU model. After the one-line model has completed its simulations, the GIS-based framework converts the histogram of beach levels at nodes backed by seawalls into sea defence toe levels required by RASP-SU. Probabilistic overtopping analysis is undertaken via Monte Carlo simulation, whereby random samples of input histograms of toe level, crest level, ground level and condition grade produce an output histogram of overtopping rates for a wide range of extreme coastal storm events (of return periods ranging typically from 1 to 1000 years). RASP-SU then analyses information on overtopping volumes, floodplain levels, performance of flood defence assets, flood spreading parameters, and flood damage at given depths to produce distributions of flood likelihood, event depth, and expected annual damage (EAD). Direct assessment of the economic risk of flooding is thereby made according to uncertainty in beach volume.

Model integration permits analysis of the wider consequences of shoreline management decisions by evaluating potential impacts of shore protection schemes (such as groynes, seawalls, beach nourishment, and mining) and changes in event-based fluvial sediment discharge on shoreline evolution, cliff erosion risk, and flood risk.

7.2 Integrated model: Holderness case study

The Holderness coastline extends between Flamborough Head and Spurn Point on the east coast of the U.K. (Figure 11). From Bridlington to Kilnsea, the Holderness coastline experiences very high rates of erosion, with approximately 1,000 hectares lost in the past 900 years, due to weakly consolidated boulder clay outcropping at sea level and cliff erosion taking place by destabilization (Wingfield and Evans, 1998). In a detailed study based on Ordnance Survey maps, Valentin (1971) found that the average cliff recession rate was 1.2 m per year, with the rate increasing southwards in response to energy input from wave action from the north. The Holderness cliff recedes intermittently and irregularly as a series of bights. Most of the cliff line is unprotected by coastal defences. Where there are defences (e.g. at Withernsea and Hornsea) rates of erosion have been locally reduced, and groyne systems have been successful in capturing sand and maintaining beach levels

The integrated UnaLineaProb and RASP-SU modelling system is now applied to the Holderness Coast within the GIS framework developed by Stripling and Panzeri (2009). The UnaLinea model domain covered about 50 km of the coastline. Model parameters include a grid spacing of 50 m, a time step of 1 day, and total duration of 20 years. Each CBU was assigned identical unstable cliff and relaxation cliff slope parameters. Cliff elevation was derived from light detection and ranging (LiDAR) data provided by the EA. Locations of the cliff toe line, seawalls, embankments, groynes, and other structures were obtained from detailed aerial photography. It should be noted that the model results presented here are purely for demonstration purposes, no extensive calibration having been undertaken; the examples are

indicative in demonstrating the flood-risk capability of the integrated model. Net littoral drift is assumed to be in the southward direction.

7.2.1 Derivation of wave climate

A back-tracking ray model was used to hindcast 13 years of 3-hourly wave climate data based on wind observations at Gorleston from 1978 to 1991. These data were further processed to provide 13 year-long time-series of daily morphological events, used to drive UnaLineaProb. To represent local conditions at regional-scale, UnaLinea permits multiple offshore wave points to be considered and hence the wave conditions to be interpolated along the coastline. For the present proof-of-concept application, the resulting morphological events are assumed constant in space (though variable in time); this may lead to some unexpected behaviour of the shoreline.

7.2.2 Construction of model domain

Figure 12 shows the model domain and backshore characteristics of the Holderness coast. Model input data included sediment size distribution, water levels, extreme overtopping rates (Environment Agency's MDSF2 National Coastal Loads Database, HR Wallingford 2008b), beach gradients, berm levels, initial shoreline position, initial cliff-top position, cliff elevation, groyne locations, seawall locations and flood-spread model Impact Zones, cell and neighbourhood volumes, property data, and depth-damage tables.

Figure 13 illustrates the GIS representation of typical backshore subsets of existing short and long groynes at Hornsea, which are engaged as required in the integrated regional model once registered within the GIS.

FIGURE 12

FIGURE 13

Figure 14 presents a flow chart of the probabilistic shoreline evolution modelling procedure in conjunction with RASP-SU. Together, these elements support the assessment of erosion and flood risk, with model builds and runs initiated locally from forms accessed within GIS.

FIGURE 14

The modelling sequence includes a coastal model, with cliff erosion and backshore toe level analysis, coupled with a flood-risk model. Pre-processing was undertaken primarily using ArcGIS standard tools, with RASP pre-processing used to build the RASP-SU models (i.e. HR Wallingford's ACCDATA program used to construct the rapid flood spreading model (RFSM) topographic model elements (Gouldby *et al*, 2008) and Economic pre-processing program to create depth-damage input tables (HR Wallingford 2008a). Model input data were organised in two databases: an ESRI Personal Geodatabase for coastal model data, model configuration variables, and default parameters; and a SQL server database for RASP-SU data. To run the model, the User first specifies which database to use, and is then guided by a Graphical User Interface (GUI). Once the run has been initiated, the GIS software controls the model operation, and manages the results. On completion of the run, the model results are added to the GIS map enabling rapid visualisation of shoreline and cliff positions,

defence toe levels, overtopping volumes, Impact Zone depth, damage, and risk. Output statistics are stored in the database to facilitate analysis of uncertainty.

Model findings presented here are based on a single-scenario test, and relate to the statistical behaviour of a groyned shoreline as a first line of defence. This defence is then backed by a mixture of seawall and soft-cliffs, and the cliffs interact with the beach through event-based failures. The statistical performance of the seawall as a defence is then examined, and the results from the risk-analysis are mapped for dissemination.

Figure 15 shows a portion of the probabilistic shoreline model results at the southern end of the Hornsea defences. The mean shoreline position at the end of each 10-year realisation is shown together with the minimum and maximum shoreline positions occurring during the convergence of the model. Where the shoreline passes landwards of a seawall, this shoreline is considered virtual, and indicates a lowering of the beach level at the seawall itself rather than a recession of the tracked contour.

FIGURE 15

The terminal groyne at the southern end of Hornsea appears to induce localised shoreline recession, and possible beach lowering where there is insufficient beach volume and the potential for cliff recession. The modelled littoral drift regime indicates beach volume continuity is maintained, thus affording natural protection to the cliff further south where the beach volume is seen to increase. Figure 16 shows how the shoreline response could expose the cliff to the possibility of failure, with localised recession of the soft-cliff evident in this vicinity. The volume of material lost from the cliff is added to the beach, and this, together with the modelled littoral

drift regime, is sufficient to sustain adequate beach volume further south, preventing significant recession of the cliffs there.

FIGURE 16

Figure 17 shows topographic model elements used by the Rapid Flood-Spreading Model (RFSM), which was developed for the Thames Estuary 2100 (Mulet-Marti and Sayers, 2006) and used to support the NaFRA 2008 study (Gouldby *et al*, 2008). The Figure has been enhanced using EA's LiDAR terrain data revealing the low lying nature of Hornsea. Also apparent in Figure 17 is a more extensive view of the shoreline behaviour at Hornsea, and where the shoreline is seen to travel landwards of the seawall, indicative of a long-term tendency for lowering of beach toe levels.

FIGURE 17

The RFSM domain extends through Hornsea, and is bounded to the north south and west by higher ground. The domain is divided into Impact Zones (Figure 18a) and bounded in the east by a seawall. By way of an example of the data output from the probabilistic simulation, the results for Impact Zone IZ 471 are now examined in detail. Figure 18b shows the properties in the model database, and defines defence lengths. Each coastal model node is assigned its own defence length, and so carries its own dedicated description of the statistical behaviour of the beach. Figure 18c presents, as an example, the derived mean beach toe level for defence lengths likely to affect flooding of IZ 471, indicating in this instance that the beach volume is accumulating with time. The database now holds significant statistical data fields

based on the probabilistic model runs, and can be queried in accord with proprietary GIS methods.

Figure 19a presents the mean flood depths for Impact Zones in the vicinity of and including IZ 471 obtained using the integrated model. In terms of structured uncertainty (within RASP-SU), this scenario represents certainty in all parameters except the level of the beach at the toe of the seawall. Here, the uncertainty of this parameter is contained within the histogram of toe-levels obtained from the probabilistic simulation of the shoreline behaviour. The GIS database records values of flood depth at various return periods as well as minimum, maximum and standard deviation values for all Impact Zones. Figure 19b shows the expected annual damage (EAD) estimated using the integrated RFSM for the locality of Impact Zone IZ 471.

FIGURE 18

FIGURE 19

8 Conclusions

A rapid, stable and accurate deterministic one-line model, UnaLinea, has been developed that is able to predict the future evolution of a shoreline at regional scale. The model is designed for probabilistic applications involving multiple realisations of shoreline evolution through Monte-Carlo sampling, driven by event-based sediment loading from cliff-falls and fluvial processes, and can include beach nourishment and artificial barriers to longshore drift. Uncertainty in beach toe-levels, a key influence on over-topping rates, is considered in the flood-risk assessment. The integrated model was set up within a dynamically-linked standalone GIS modelling framework

(see Stripling *et al*. 2007 and Stripling and Panzeri 2009), allowing generation of long duration time-series of wave data (over decades) and subsequent derivation of morphologically-averaged conditions.

The UnaLinea model was applied to a site on the west coast of Calabria, Italy; the results indicated that shoreline response would be predominantly erosive, based on present-day sediment input conditions. It was predicted that a fivefold increase in fluvial loading would prove ineffective at preventing coastal erosion, whereas artificial beach nourishment could effectively manage the erosion-risk. In terms of coastal management, the ease by which scenarios can be examined using a fast GIS system with embedded probabilistic modelling means that it is feasible in practice to ascertain the potential impacts of a multitude of intervention options.

An integrated modelling system that permits joint assessment of flood and erosion risk was applied to a 50 km length of the Holderness shoreline on the east coast of England. Broad 'sediment cell' scale was incorporated, allowing impact of natural or man-made change to the shore to be assessed within the flood risk model. Modelling was undertaken probabilistically, allowing uncertainty, stochastic events, and non-linear responses to be considered, year-on-year, enabling evaluation of flood risk evolution and providing evidence to support confidence in the assessment. Such integrated modelling systems could prove to be extremely valuable tools in coastal zone management.

Acknowledgements

This research was performed as part of the Flood Risk Management Research Consortium funded by the UK Engineering and Physical Sciences Research Council under grant GR/S76304/01 with co-funding from the Environment Agency, Rivers

Agency Northern Ireland and Office of Public Works, Ireland. Due to the confidential nature of some of the research materials supporting this publication not all of the data can be made accessible to other researchers. Please contact info@hrwallingford.com for more information. The authors are grateful to Nigel Pontee and Rob Haddon (Halcrow Group plc) who contributed to the analysis, Giovanni Ricca (Autorità Bacino Regione Calabria) for his foresight and support, and Neil McClachlan (East Riding of Yorkshire Council) for data supplied from the Coastal Explorer web-site. Alistair Borthwick would like to thank the University of Oxford and Stuart Stripling would like to thank HR Wallingford, where they were based previously and where part of the work reported herein was undertaken. Dani Goldberg and David Wyncoll provided valuable input to model development whilst they were at HR Wallingford. Ilektra-Georgia Apostolidou, Alan Brampton, Paul Taylor, and Richard Soulsby contributed to the one-line model development through a Knowledge Transfer Secondment between the University of Oxford and HR Wallingford.

References

Bakker W.T., Klein Breteler E.H.J. and Roos A. (1970) The dynamics of a coast with a groyne system. Proc. 12th Int. Conf. on Coastal Engrg, ASCE, 1001-1020.

Balson P., Tragheim D. and Newsham R., (1998) Determination and prediction of sediment yields from recession of the Holderness coast, eastern England. Proc., 33rd MAFF Conference of River and Coastal Engineers, Keele, Pp 4.5.1–4.5.11.

Bates P.D., Dawson R.J., Hall J.W., Horritt M.S., Nicholls R.J., Wicks J. and Hassane M.A.A.M. (2005) Simplified two-dimensional modelling of coastal flooding for risk assessment and planning. Coastal Engineering, 52(9): 793-810.

Bedford T. and Cooke R. (2001) Probabilistic Risk Analysis: Foundations and Methods. Cambridge University Press, ISBN 0 521 77320 2.

CERC (1984) Shore Protection Manual. U.S. Army Corps of Engineers, Waterways Experiment Station, Coastal Engineering Research Center, Washington D.C.

Courant R., Friedrichs K. and Lewy H. (1967) On the partial difference equations of mathematical physics, IBM Journal, 11: 215-234.

Damgaard J.S. and Soulsby R.L. (1997) Longshore bed-load transport. Proc. 25th Int. Conf. Coastal Engineering, ASCE, 3, 3614-3627.

Dean R.G. and Dalrymple R.A. (2002) Coastal Processes with Engineering Applications, Cambridge University Press, Cambridge, U.K.

Falqués A. (2003) On the diffusivity in coastline dynamics. Geophys. Res. Lett., 30(21): 2119.

Fletcher C.A.J. (1990) Computational Techniques for Fluid Dynamics – Vol. 1, Springer-Verlag, New York Berlin Heidelberg.

Fotopoulos F., Makropoulos C., Mimikou M.A., (2010). Flood forecasting in transboundary catchments using the Open Modeling Interface. J.Environmental Modelling & Software, 25: 1640-49.

Gouldby, B.P., Sayers, P.B., Mulet-Marti, J., Hassan, M. and Benwell, D (2008) A Methodology for Regional Scale Flood Risk Assessment. Proceedings of the ICE - Water Management, 161 (3). (2008)

Gouldby B.P., Sayers P. B., Panzeri M. C. and Lanyon J. E. (2010) Development and application of efficient methods for the forward propagation of epistemic uncertainty and sensitivity analysis within complex broad-scale flood risk system models. Canadian Journal of Civil Engineering, 37(7): 955-967.

Hall J.W., Dawson R.J., Sayers P., Rosu C., Chatterton J., Deakin R. (2003) A

methodology for national-scale flood risk assessment. Proceedings of the Institution of Civil Engineers - Water & Maritime Engineering 2003, 156(3), 235-247.

Hanson K. and Kraus N.C. (1989) GENESIS – generalized model for simulating shoreline change, Volume 1: reference manual and users guide. Tech Rep CERC-89-19, USAE-WES, Coastal Eng Research Centre, Vicksburg, Miss., USA.

Horikawa K. (1988) Nearshore Dynamics and Coastal Processes, University of Tokyo Press, Tokyo, Japan.

HR Wallingford (2008a). NaFRA 2007 Technical Note MCR5289-RT009: Economic Calculations

HR Wallingford (2008b). Report EX5677: NaFRA 2007 Main Phase: Refinement of joint probability regions.

HR Wallingford (2009) Report EX5953: Understanding and communicating uncertainty in the NaFRA 08 output.

Komar P.D. (1998) Beach Processes and Sedimentation, Prentice-Hall, Inglewood Cliffs, New Jersey.

Kraus N.C. and Harikai S. (1983) Numerical model of the shoreline change at Oarai beach, Coastal Engineering, 7(1):1-28.

Larson M., Hanson H. and Kraus N.C. (1987) Analytical solutions of the one-line model of shoreline change. Tech. Report CERC-87-15, U.S. Army Corps of Engineers, Coastal Engineering Research Center, Vicksburg, Miss., USA.

Le Méhauté B. and Soldate M. (1977) Mathematical modelling of shoreline evolution. Misc. Report 77-10, U.S. Army Corps of Engineers, Coastal Engineering Research Center, Vicksburg, Miss., USA.

Lee E. M. and Clark A. R. (2002) The Investigation and Management of Soft Rock Cliffs, published by Thomas Telford (ISBN 07277-3110-6)

McGahey C. and Sayers P B. (2008) Long term planning - Robust strategic decision making in the face of gross uncertainty tools and application to the Thames. In Flood Risk Management: Research and Practice. Edited by Samuels P, Taylor & Francis Group, London.

Mulder, J.P.M. and Tonnon , P.K (2010) Sand Engine: Background and design of a mega nourishment pilot in the Netherlands, Proc. Coastal Engineering Conference

Mulet-Marti J. and Sayers P.B. (2006) Thames Estuary 2100: Rapid flood spreading methodology (RFSM). Report for TE2100 project Technical Note DT4.

Murray A.B. and Ashton A. (2003) Sandy-coastline evolution as an example of pattern formation involving emergent structures and interactions. Proc. Int. Conf. on Coastal Sediments 2003. CD-ROM published by World Scientific Publishing Corp. and East Meets West Productions, Corpus Christi, Texas, USA. ISBN 981-238-422-7.

Ohl C., Frew P., Sayers P.B., Watson G., Lawton P., Farrow B.J., Walkden M., Hall J. (2003). North Norfolk – a regional approach to coastal erosion management and sustainability in practice. Proceeding of the ICE International Conference on Coastal Management, Brighton, UK 2003

Ozasa H. and Brampton A.H. (1980) Mathematical modelling of beaches backed by seawalls. Coastal Engineering, 4(1): 47-63.

Panzeri M, Stripling S., Chesher T. (2012) A GIS Framework for Probabilistic Modelling Coastal Erosion and Flood-Risk. Proceedings of PIANC - COPEDEC VIII. Madras, India, 20-24 February, 2012.

Pelnard-Considère R. (1956) Essai de théorie de l'évolution des formes de rivage en plages de sable et de galets. Société Hydrotechnique de France, IV^{es} Journées de l'Hydraulique, Les Energies de la Mer, Paris, Question 3, Rapport No. 1, Societe Hydrotechnique de France: 289- 298.

Reeve D. (2006) Explicit expression for beach response to non-stationary forcing near a groyne. Journal of Waterway, Port, Coastal and Ocean Engineering, ASCE, 132(2): 125-132.

Reeve, D., Chadwick A., Fleming C. (2004) Coastal Engineering: Processes, Theory and Design Practice, SPON Press, Taylor & Francis, London and New York.

Roach P. J. (1998) Verification and Validation in Computational Science and Engineering, Hermosa Publishers, Albuquerque, New Mexico, USA

Sayers P. B. and Meadowcroft I. C. (2005) RASP - A hierarchy of risk-based methods and their application. 40th Defra Flood and Coastal Management Conference, York, U.K.

Soulsby (1997) Dynamics of Marine sands, Thomas Telford, London.

Stripling S., Panzeri M., Kemp J. and Brampton A. (2007) Broad-scale morphodynamic shoreline modelling within a standalone GIS coastal management tool: GTI-SEAMaT, Proc. I.C.E. Int. Conf. on Coastal Management, 31 October - 1 November 2007,119-129.

Stripling S. and Panzeri M.C. (2009) Modelling shoreline evolution to enhance flood risk assessment, Proc. I.C.E. Maritime Engineering, 162(3):137-144.

Swart D.H. (1976) Predictive equations regarding coastal transport. Proc. 15th Coastal Engineering Conference, Vol II, Chapter 66, 1112-1132.

Tonnon P. Stam G. Huisman B. van Rijn L, 2014. Initial Sand losses and life span predictions for mega-nourishments along the Dutch coast. Coastal Engineering

Proceedings 01/2014; 1(34):45

Valentin H. (1971) Land Loss at Holderness. Applied Coastal Geomorphology. Ed. Steers, J.A., MacMillan, London, pp116–137.

Del Valle R., Medina R. and Losada M.A. (1993) Dependence of Coefficient K on grain size. Tech. Note No 3062, Journal of Waterway, Port, Coastal and Ocean Engineering, ASCE, 119(5): 568-574.

Walkden M., Hall J., Meadowcroft I. and Stripling S (2000) Probabilistic process modelling of soft cliff erosion and management, Proc. 27th Int. Conf. Coastal Engineering, ASCE, Sydney, Vol 4, 3100-3113.

Walton T.L. and Chiu T.Y. (1979) A review of analytical techniques to solve the sand transport equation and some simplified solutions. Proc. Coastal Structures '79, ASCE, 809-837.

Wang B. and Reeve D. (2010) Probabilistic modelling of long-term beach evolution near segmented shore-parallel breakwaters, Coastal Engineering, 57(8):732–744.

Wingfield R. and Evans, C., (1999) The significance of the shoreface ramp for coastal development: Holderness, eastern England, UK. Proceedings of Littoral '99.

Zacharioudaki A. and Reeve D.E. (2010) A note on the numerical solution of the one-line model, Environmental Modelling & Software, 25(6):802–807.

Figure List

Figure 1

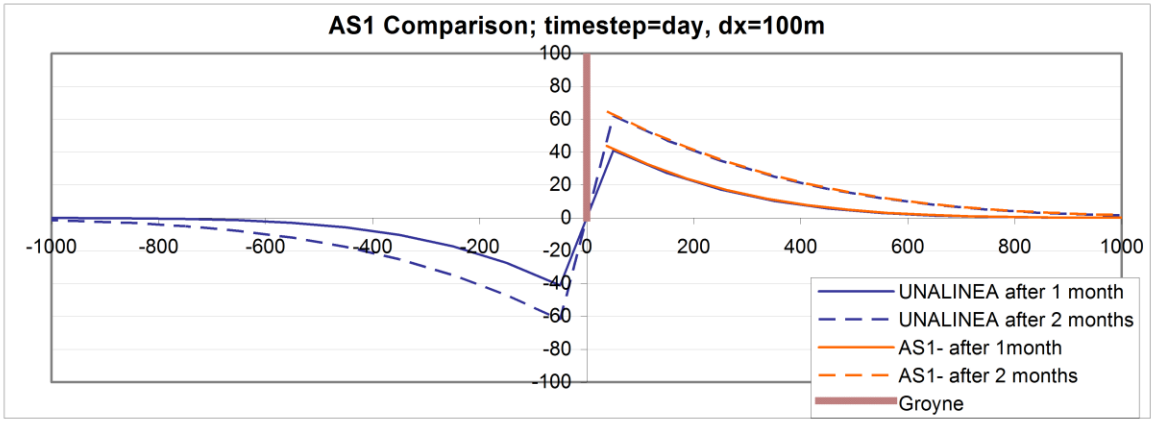
AS1 Comparison; timestep=day, dx=100m
100
80
60
40
20
0
-20
-40
-60
-80
-100
-1000
-800
-600
-400
-200
0
200
400
600
800
1000
UNALINEA after 1 month
UNALINEA after 2 months
AS1- after 1month
AS1- after 2 months
Groyne

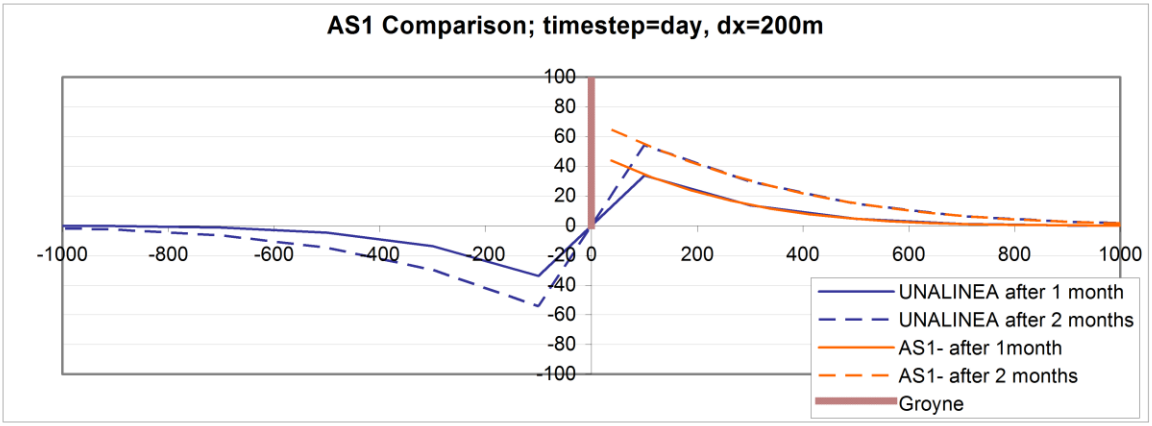
AS1 Comparison; timestep=day, dx=200m
100
80
60
40
20
0
-20
-40
-60
-80
-100
-1000
-800
-600
-400
-200
0
200
400
600
800
1000
UNALINEA after 1 month
UNALINEA after 2 months
AS1- after 1month
AS1- after 2 months
Groyne

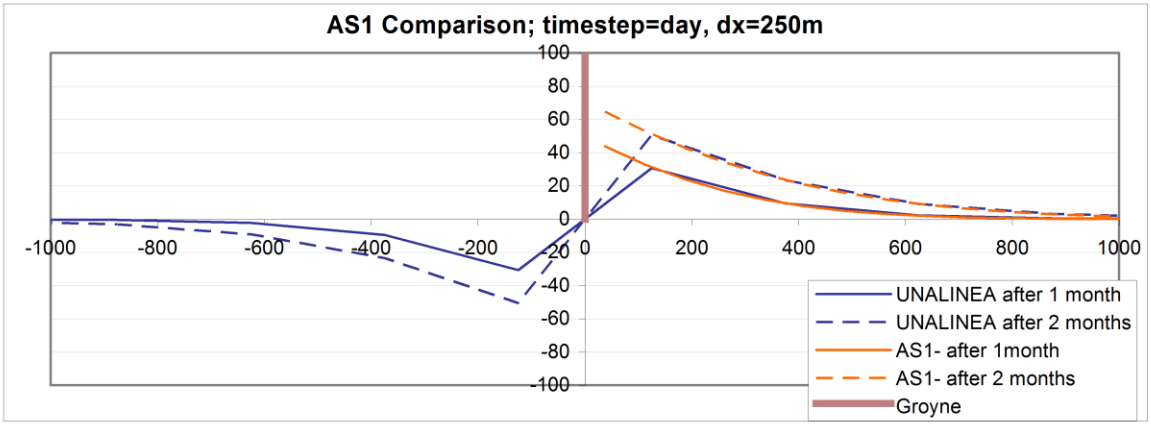
AS1 Comparison; timestep=day, dx=250m
100
80
60
40
20
0
-20
-40
-60
-80
-100
-1000
-800
-600
-400
-200
0
200
400
600
800
1000
UNALINEA after 1 month
UNALINEA after 2 months
AS1- after 1month
AS1- after 2 months
Groyne

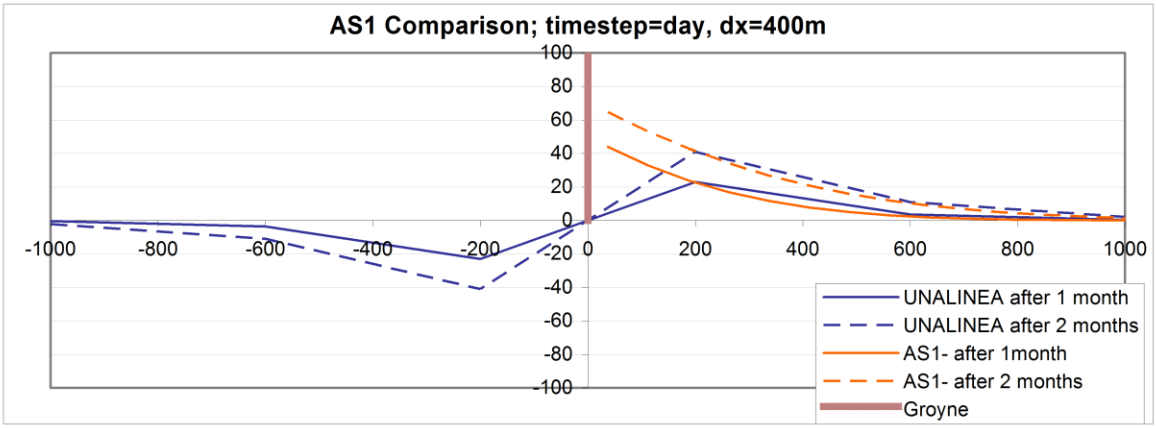
AS1 Comparison; timestep=day, dx=400m
100
80
60
40
20
0
-20
-40
-60
-80
-100
-1000
-800
-600
-400
-200
0
200
400
600
800
1000
UNALINEA after 1 month
UNALINEA after 2 months
AS1- after 1month
AS1- after 2 months
Groyne

Figure 2

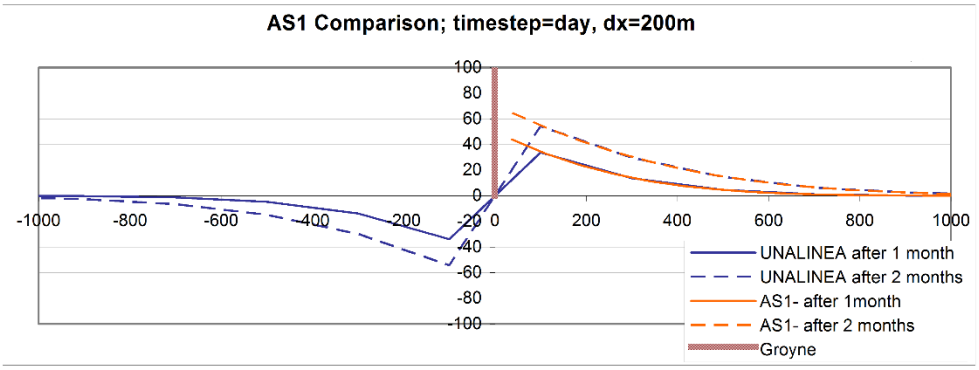
AS1 Comparison; timestep=day, dx=200m
100
80
60
40
20
0
-20
-40
-60
-80
-100
-1000
-800
-600
-400
-200
0
200
400
600
800
1000
UNALINEA after 1 month
UNALINEA after 2 months
AS1- after 1month
AS1- after 2 months
Groyne

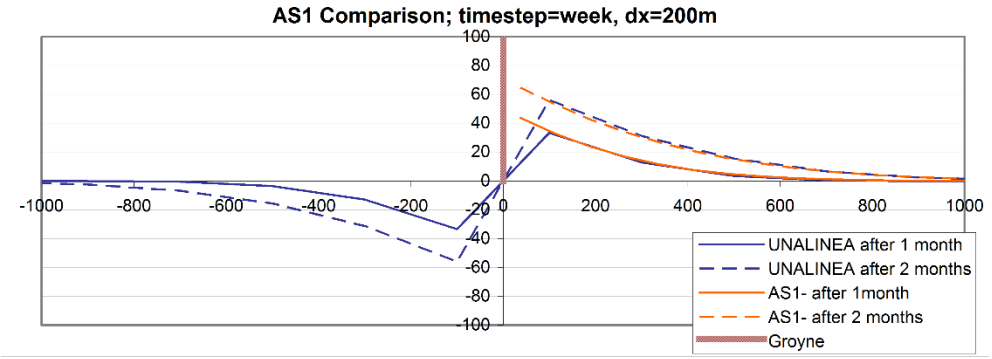
AS1 Comparison; timestep=week, dx=200m
100
80
60
40
20
0
-20
-40
-60
-80
-100
-1000
-800
-600
-400
-200
0
200
400
600
800
1000
UNALINEA after 1 month
UNALINEA after 2 months
AS1- after 1month
AS1- after 2 months
Groyne

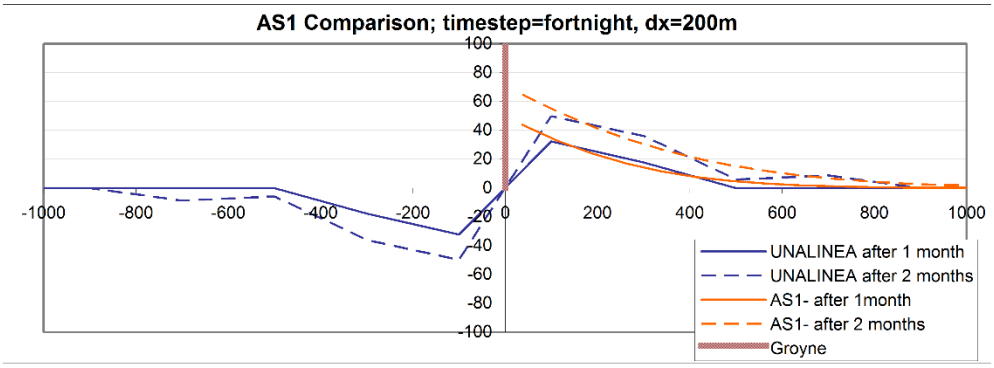
AS1 Comparison; timestep=fortnight, dx=200m
100
80
60
40
20
0
-20
-40
-60
-80
-100
-1000
-800
-600
-400
-200
0
200
400
600
800
1000
UNALINEA after 1 month
UNALINEA after 2 months
AS1- after 1month
AS1- after 2 months
Groyne

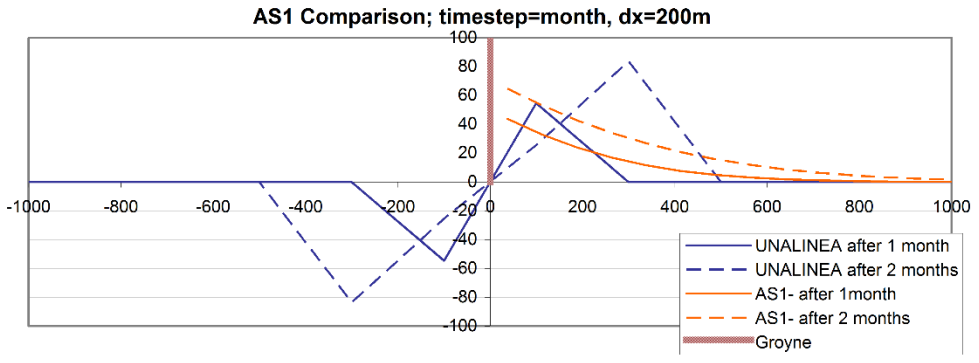
AS1 Comparison; timestep=month, dx=200m
100
80
60
40
20
0
-20
-40
-60
-80
-100
-1000
-800
-600
-400
-200
0
200
400
600
800
1000
UNALINEA after 1 month
UNALINEA after 2 months
AS1- after 1month
AS1- after 2 months
Groyne

Figure 3

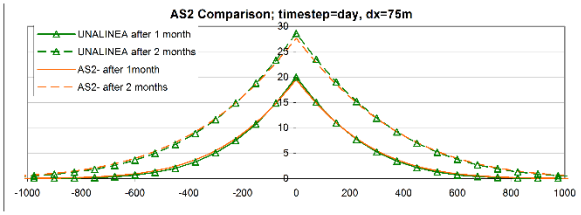
AS2 Comparison; timestep=day, dx=75m
UNALINEA after 1 month
UNALINEA after 2 months
AS2- after 1month
AS2- after 2 months

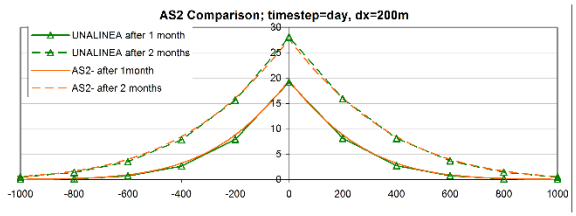
AS2 Comparison; timestep=day, dx=200m
UNALINEA after 1 month
UNALINEA after 2 months
AS2- after 1month
AS2- after 2 months

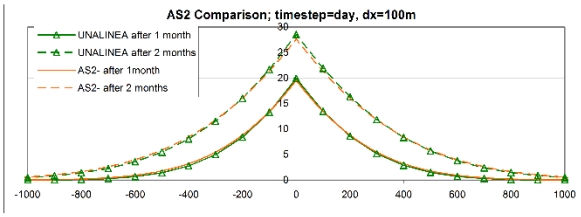
AS2 Comparison; timestep=day, dx=100m
UNALINEA after 1 month
UNALINEA after 2 months
AS2- after 1month
AS2- after 2 months

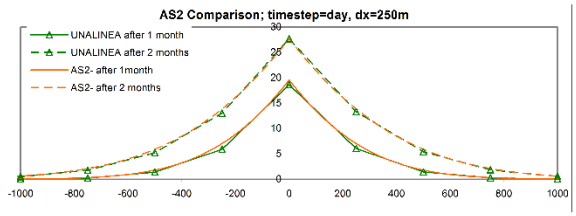
AS2 Comparison; timestep=day, dx=250m
UNALINEA after 1 month
UNALINEA after 2 months
AS2- after 1month
AS2- after 2 months

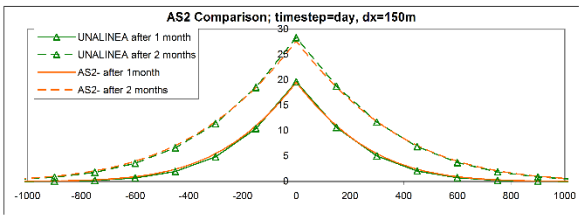
AS2 Comparison; timestep=day, dx=150m
UNALINEA after 1 month
UNALINEA after 2 months
AS2- after 1month
AS2- after 2 months

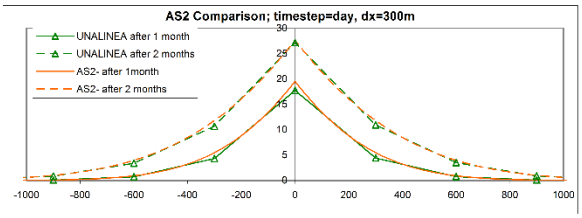
AS2 Comparison; timestep=day, dx=300m
UNALINEA after 1 month
UNALINEA after 2 months
AS2- after 1month
AS2- after 2 months

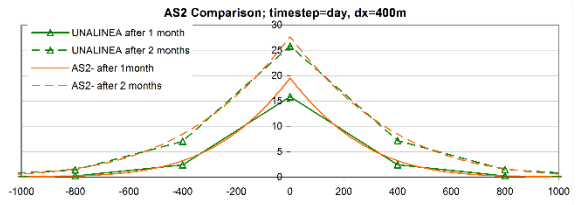
AS2 Comparison; timestep=day, dx=400m
UNALINEA after 1 month
UNALINEA after 2 months
AS2- after 1month
AS2- after 2 months

Figure 4

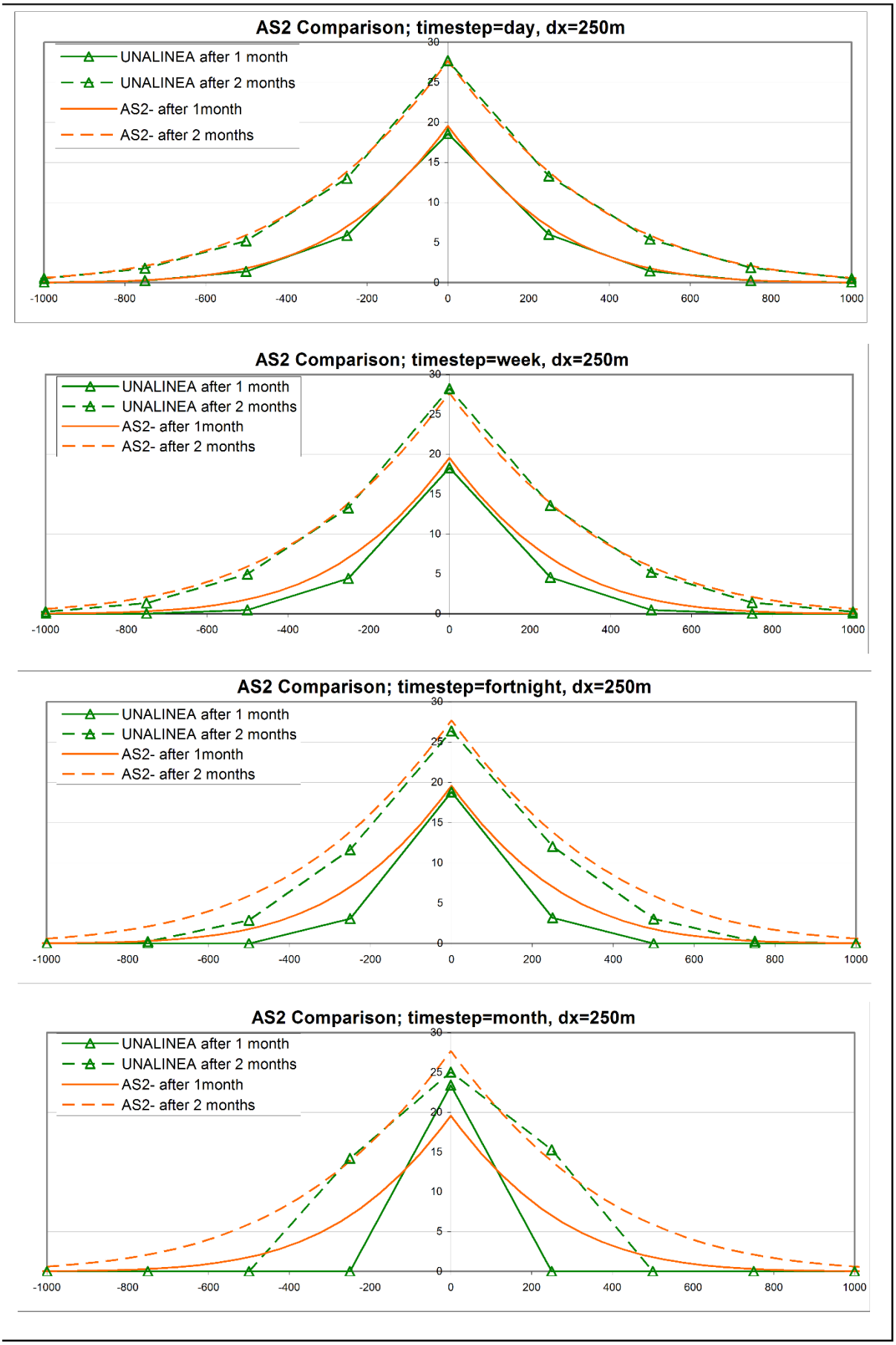
AS2 Comparison; timestep=day, dx=250m
UNALINEA after 1 month
UNALINEA after 2 months
AS2- after 1month
AS2- after 2 months
AS2 Comparison; timestep=week, dx=250m
UNALINEA after 1 month
UNALINEA after 2 months
AS2- after 1month
AS2- after 2 months
AS2 Comparison; timestep=fortnight, dx=250m
UNALINEA after 1 month
UNALINEA after 2 months
AS2- after 1month
AS2- after 2 months
AS2 Comparison; timestep=month, dx=250m
UNALINEA after 1 month
UNALINEA after 2 months
AS2- after 1month
AS2- after 2 months

Figure 5

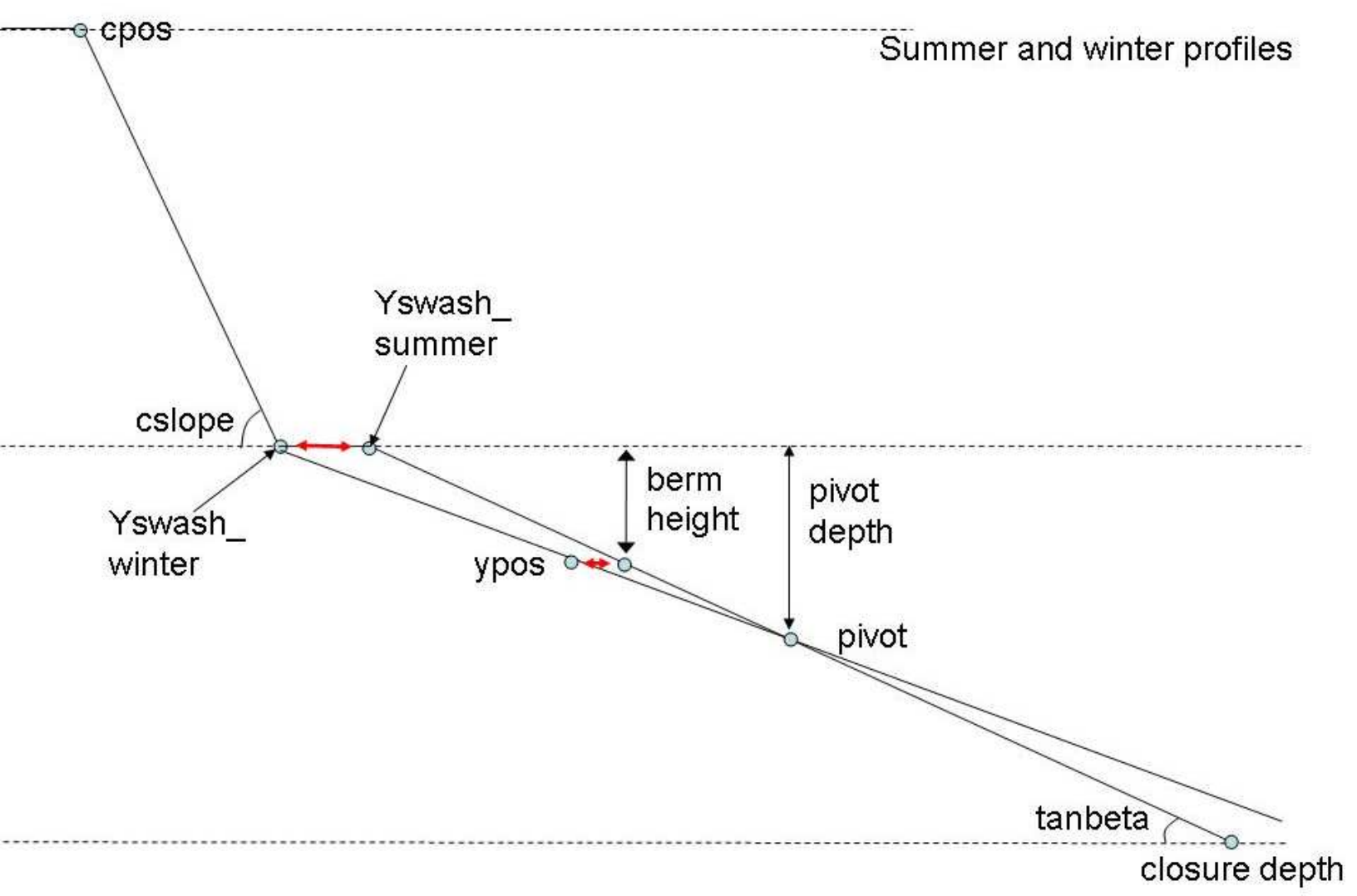
cpos
Summer and winter profiles
Yswash_
summer
cslope
Yswash_
winter
berm
height
pivot
depth
ypos
pivot
tanbeta
closure depth

Figure 6a

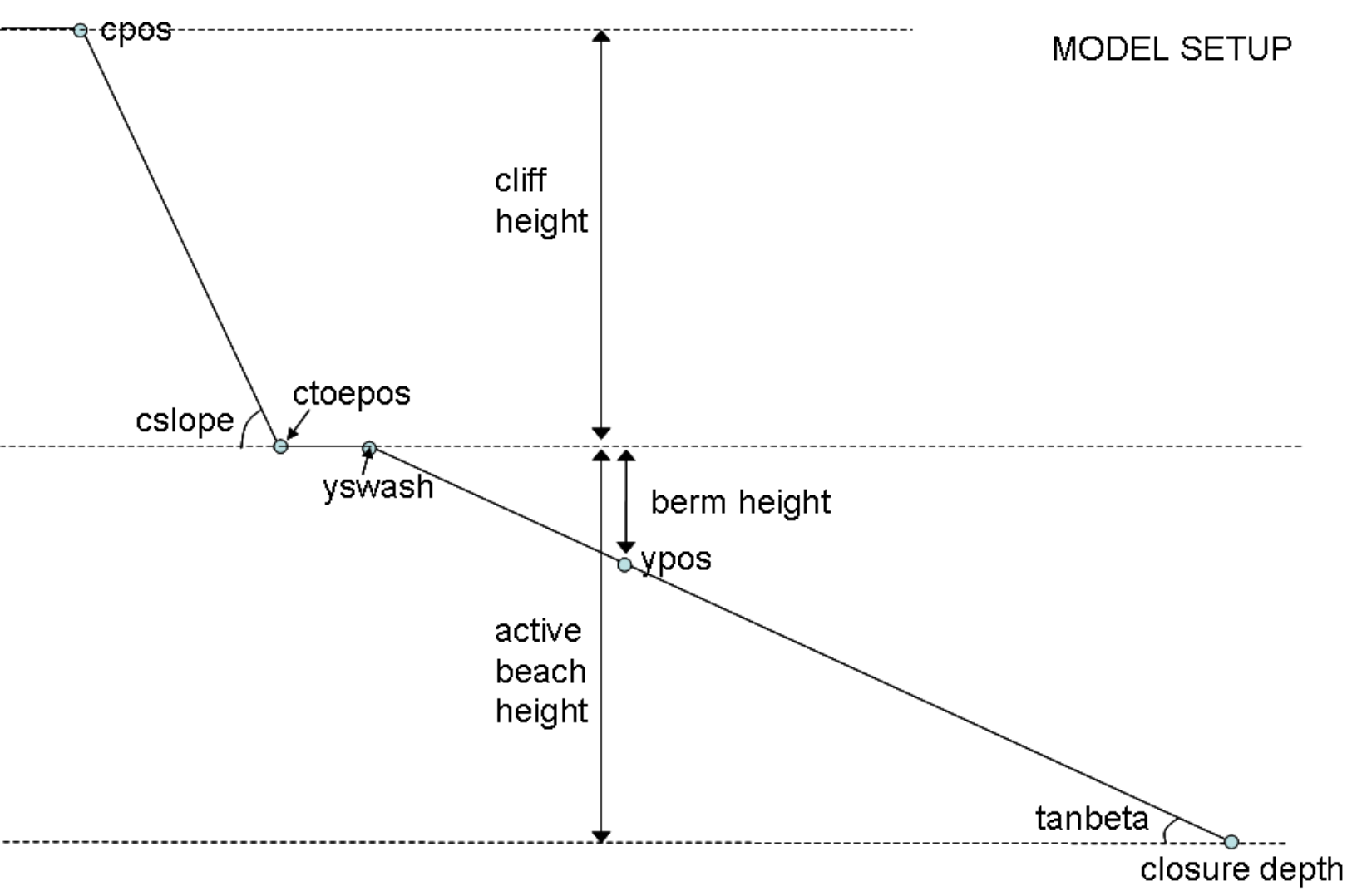
MODEL SETUP
cpos
cliff
height
ctoepos
cslope
yswash
berm height
ypos
active
beach
height
tanbeta
closure depth

Figure 6b

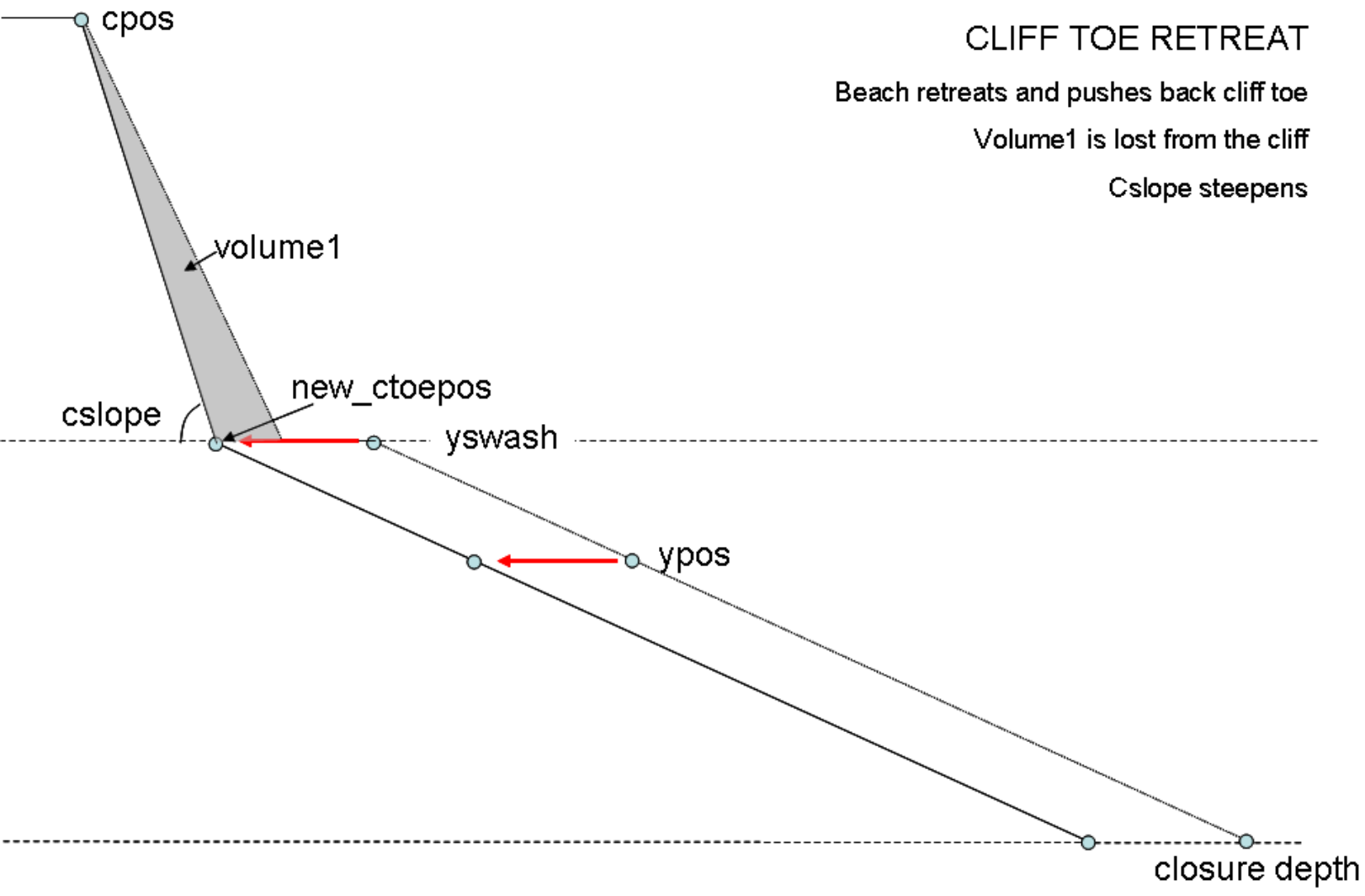
cpos
CLIFF TOE RETREAT
Beach retreats and pushes back cliff toe
Volume1 is lost from the cliff
Cslope steepens
volume1
new_ctoepos
cslope
yswash
ypos
closure depth

Figure 6c

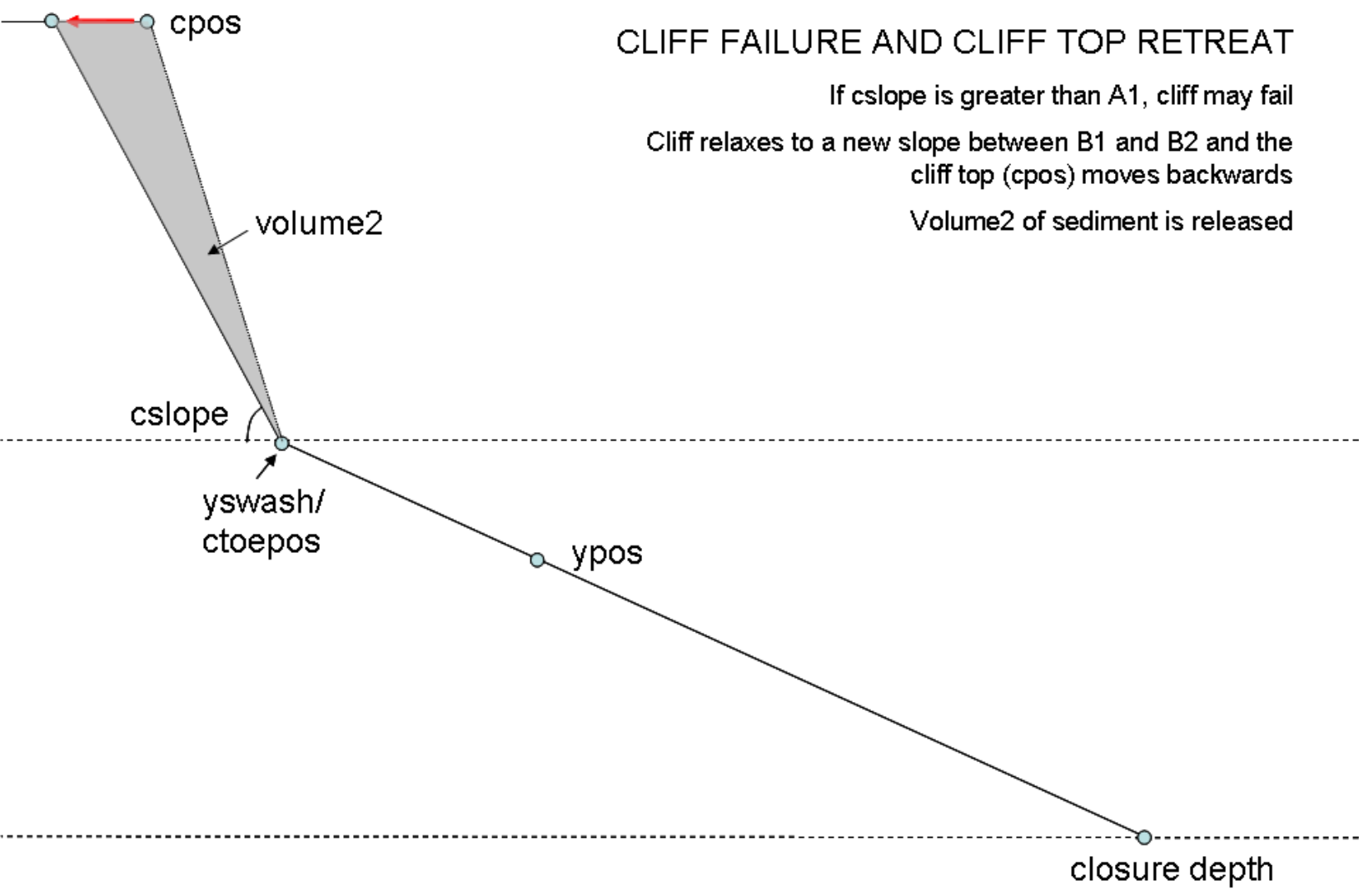
cpos
CLIFF FAILURE AND CLIFF TOP RETREAT
If cslope is greater than A1, cliff may fail
Cliff relaxes to a new slope between B1 and B2 and the cliff top (cpos) moves backwards
Volume2 of sediment is released
volume2
cslope
yswash/
ctoepos
ypos
closure depth

Figure 7

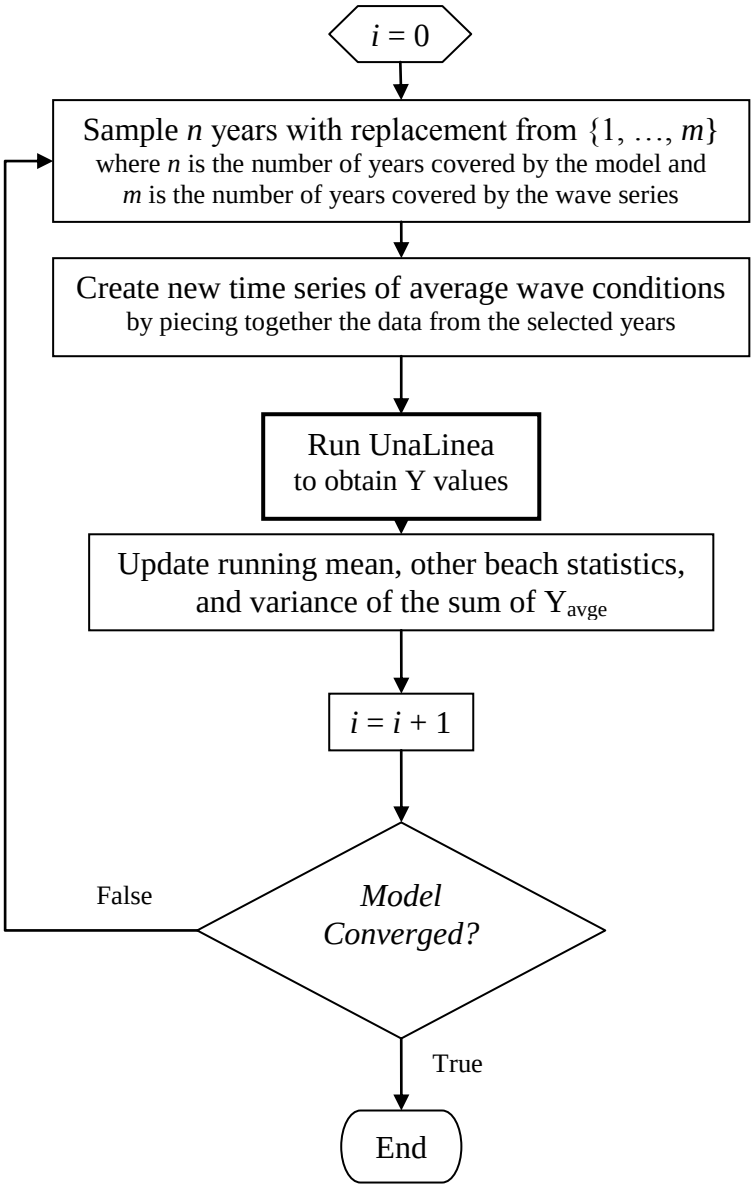
i = 0
Sample n years with replacement from {1, …, m}
where n is the number of years covered by the model and
m is the number of years covered by the wave series
Create new time series of average wave conditions
by piecing together the data from the selected years
Run UnaLinea
to obtain Y values
Update running mean, other beach statistics,
and variance of the sum of Y avge
i = i + 1
Model
Converged?
False
True
End

Figure 8

Click here to download high resolution image

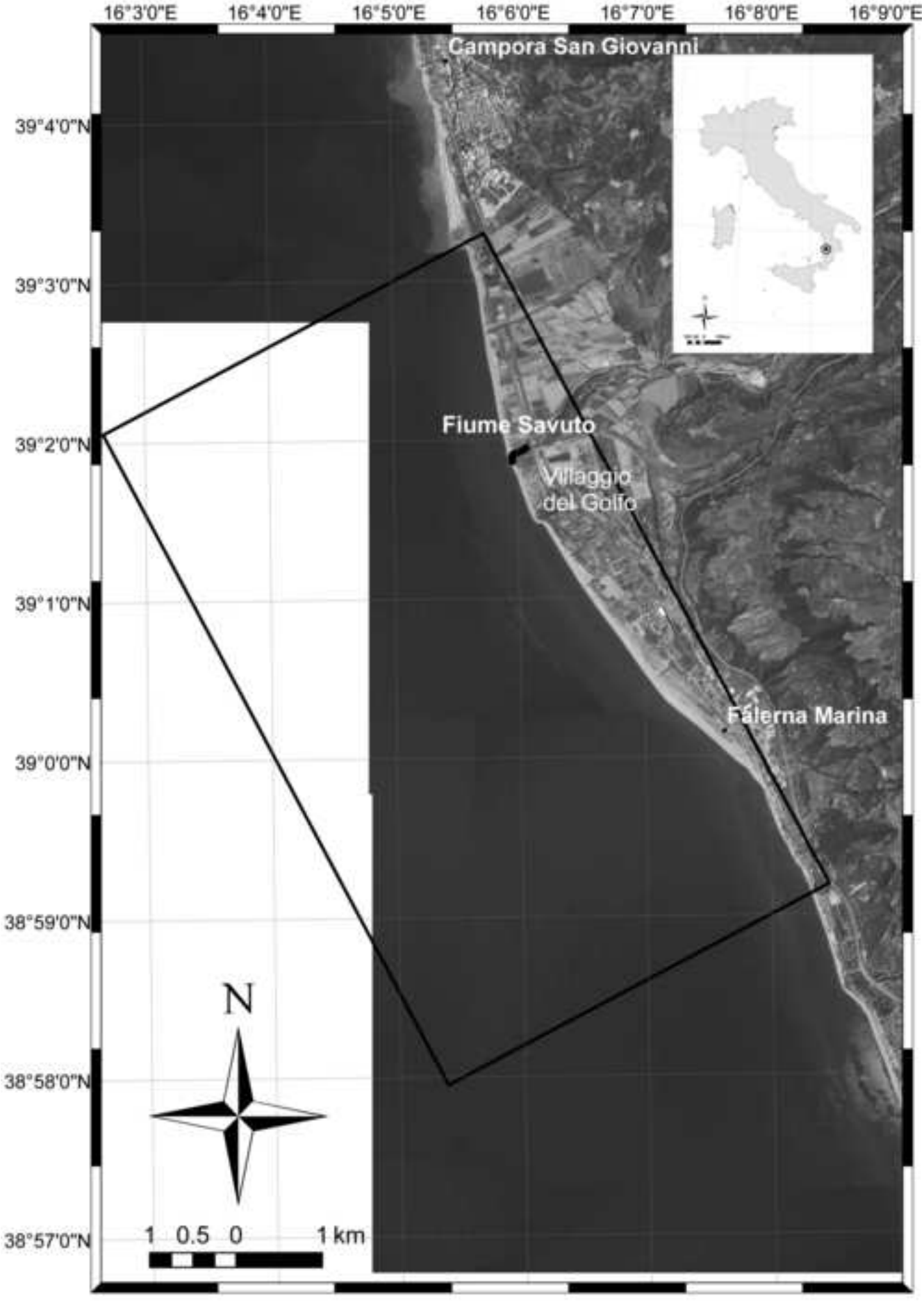

Figure 9

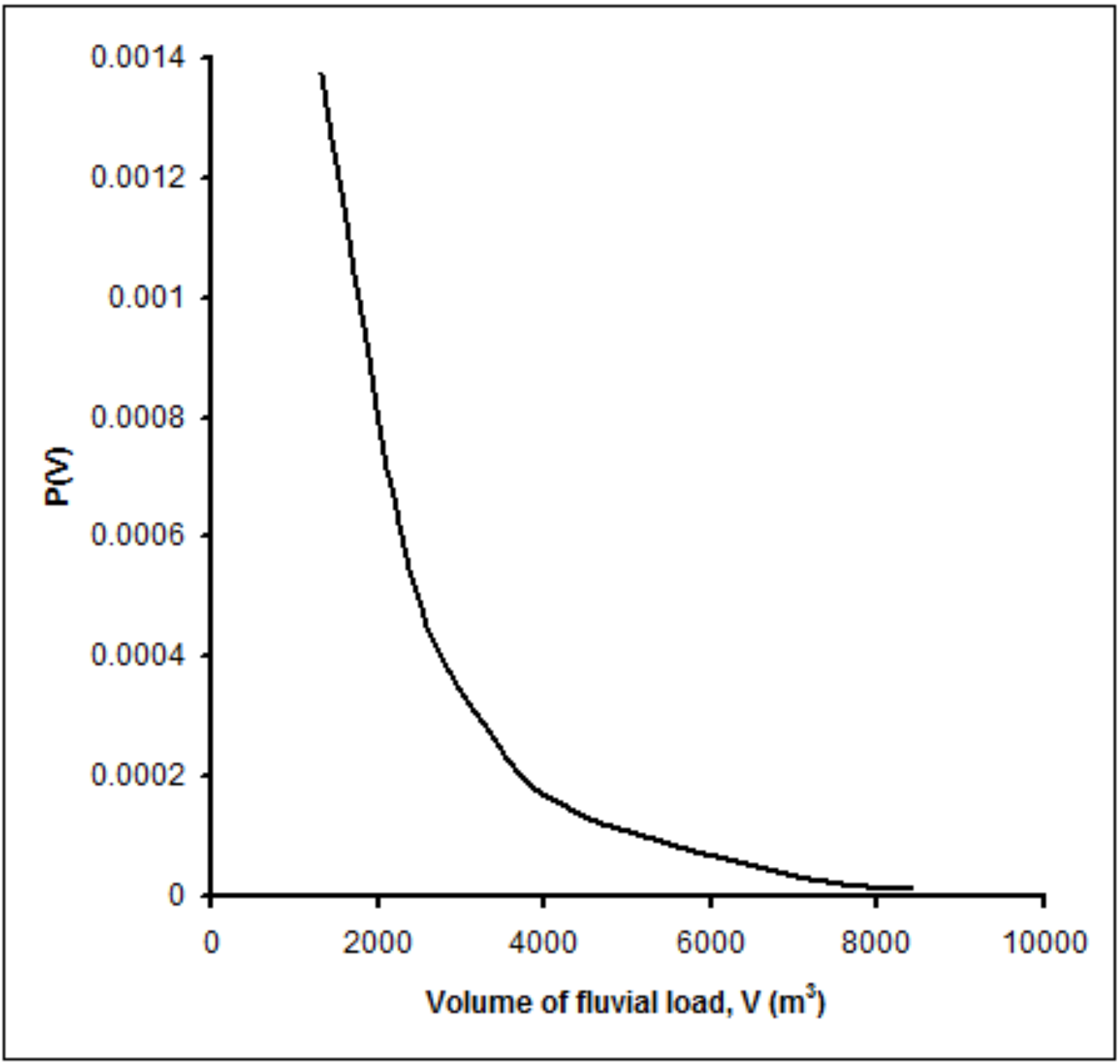
0.0014
0.0012
0.001
0.0008
0.0006
0.0004
0.0002
0
P(V)
0
2000
4000
6000
8000
10000
Volume of fluvial load, V (m3)

Figure 10a

Click here to download high resolution image

Figure 10b

Click here to download high resolution image

Figure 10c

Click here to download high resolution image

Figure 11

Click here to download high resolution image

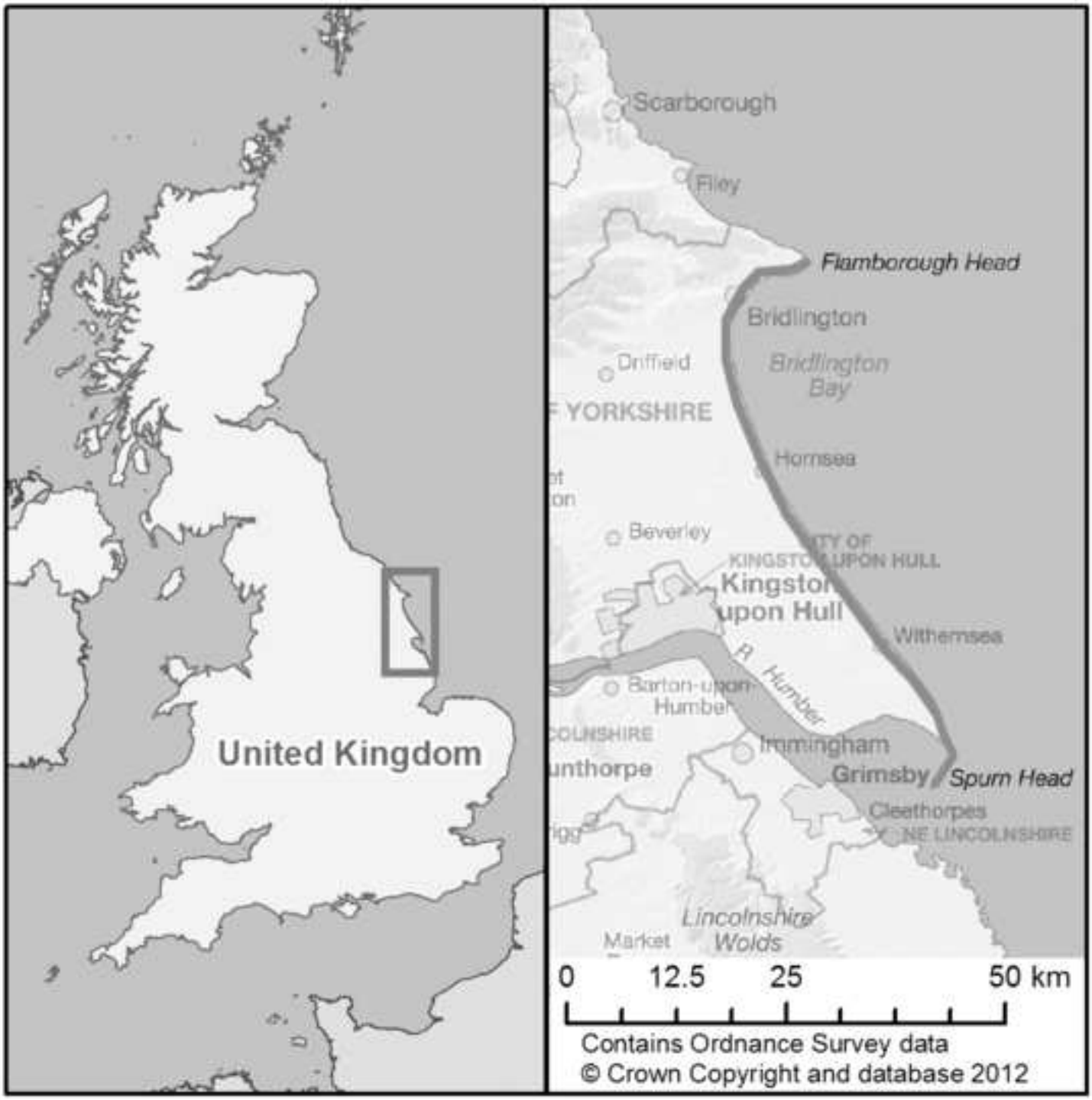

Figure 12

Click here to download high resolution image

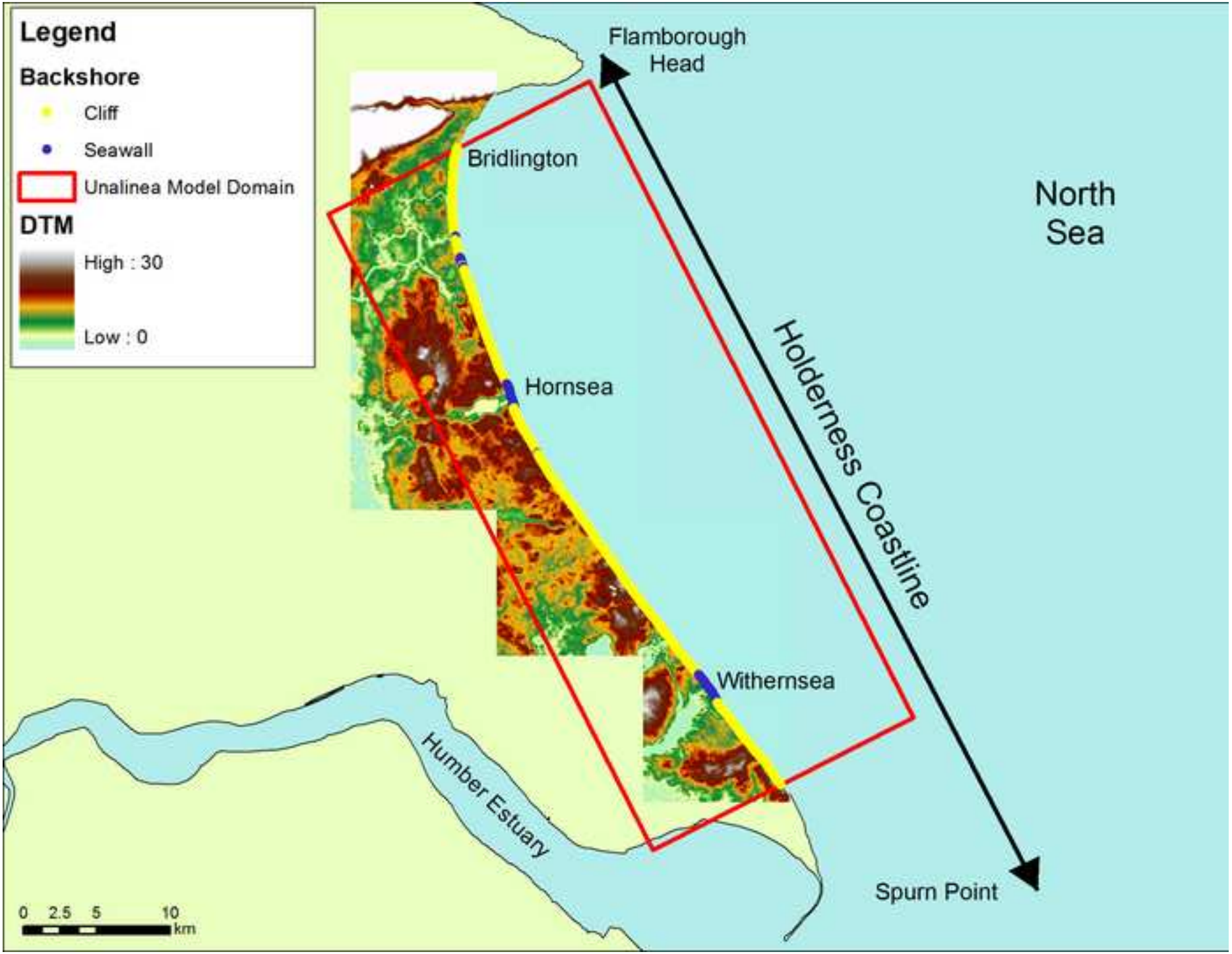

Figure 13

Click here to download high resolution image

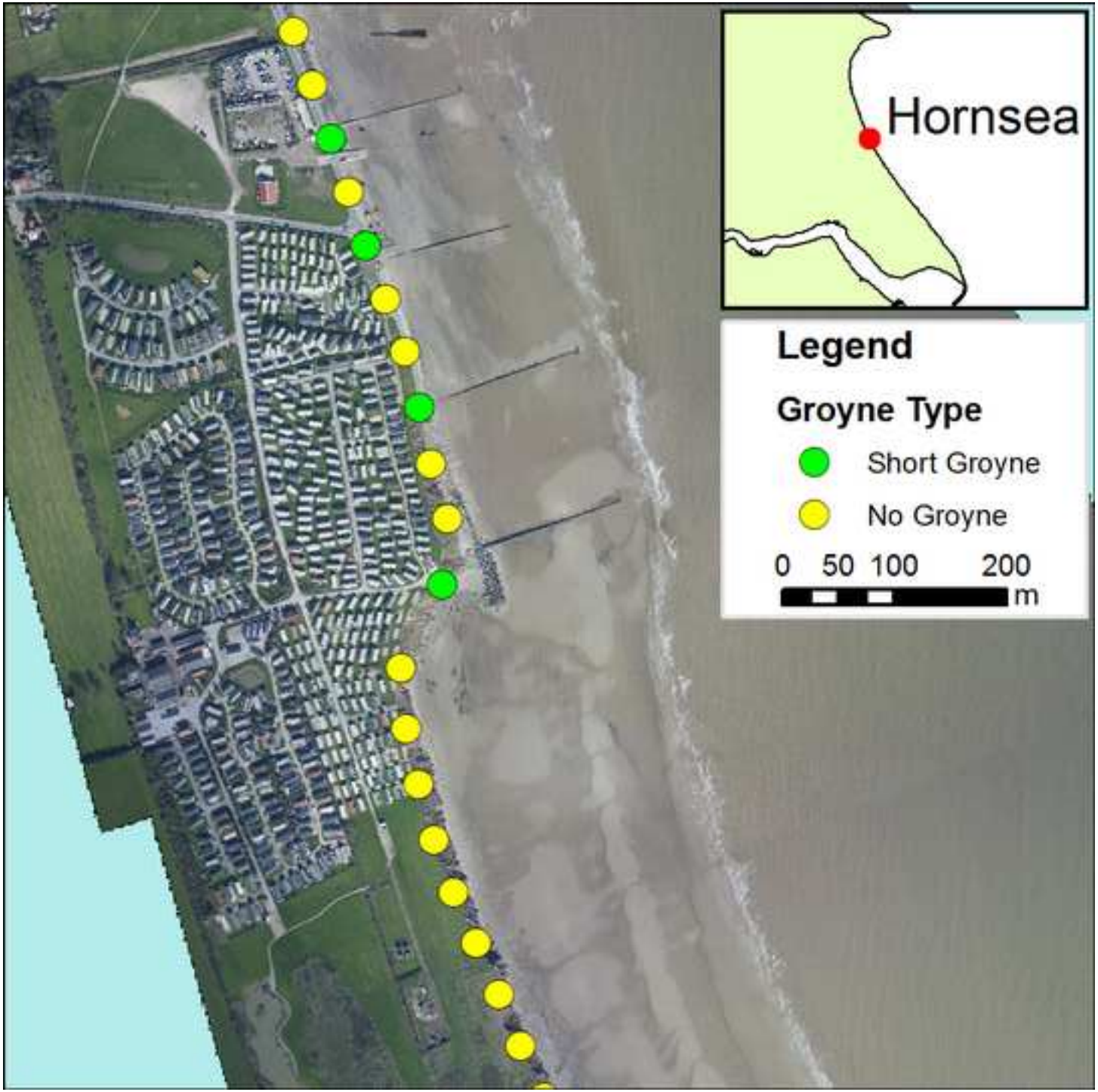

Figure 14

Click here to download high resolution image

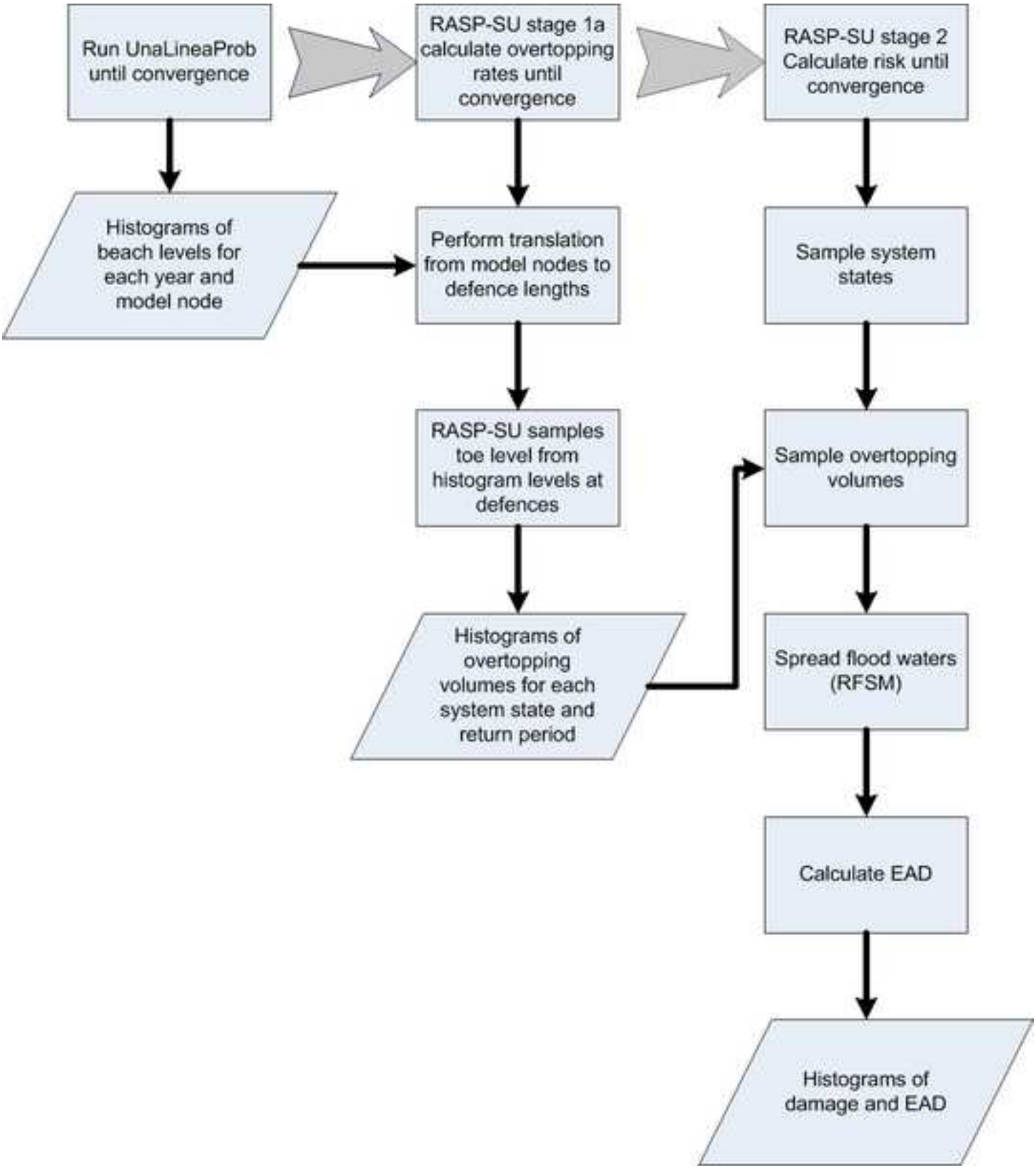

Figure 15

Click here to download high resolution image

Figure 16

Click here to download high resolution image

Figure 17

Click here to download high resolution image

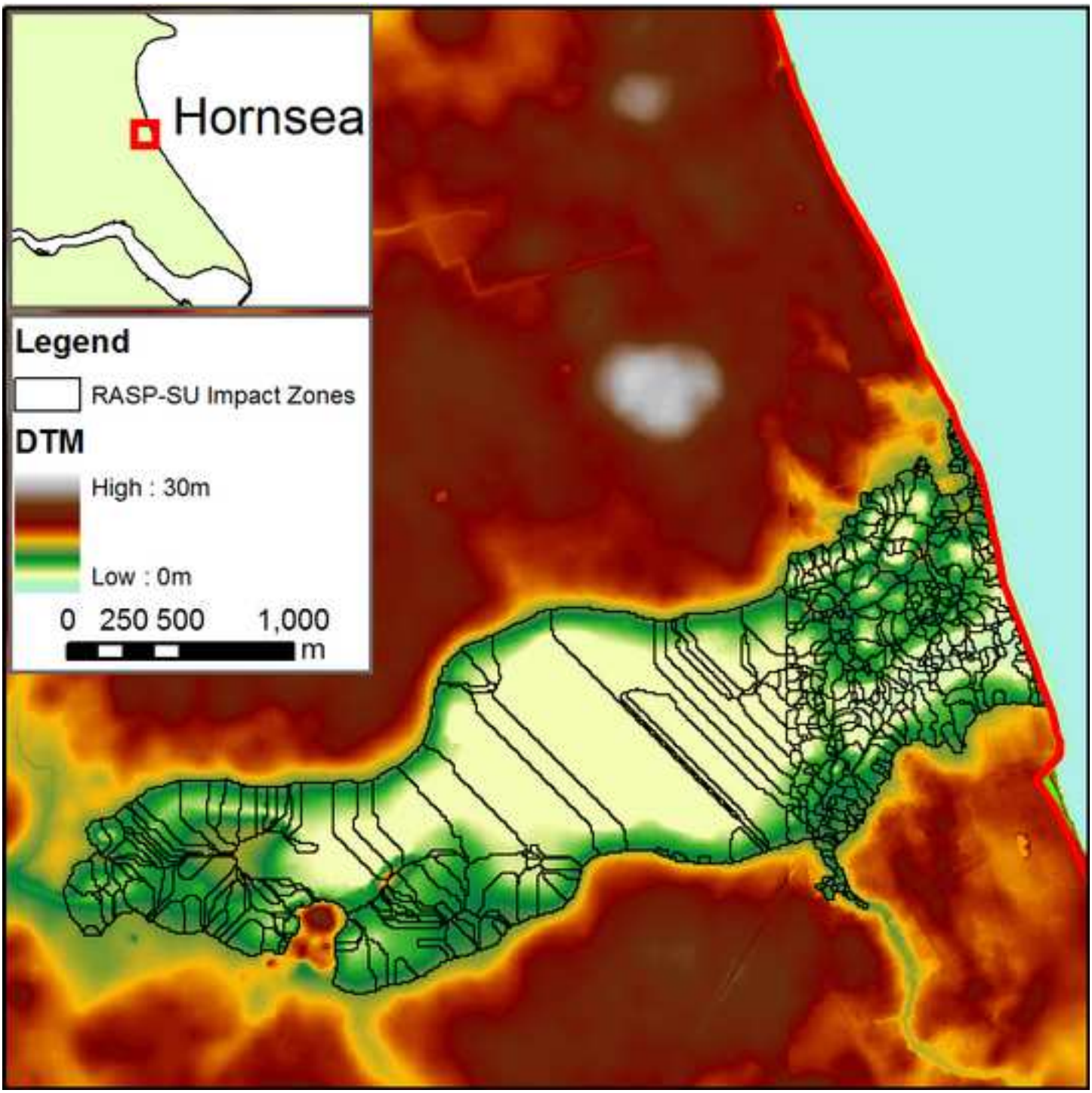

Figure 18a

Click here to download high resolution image

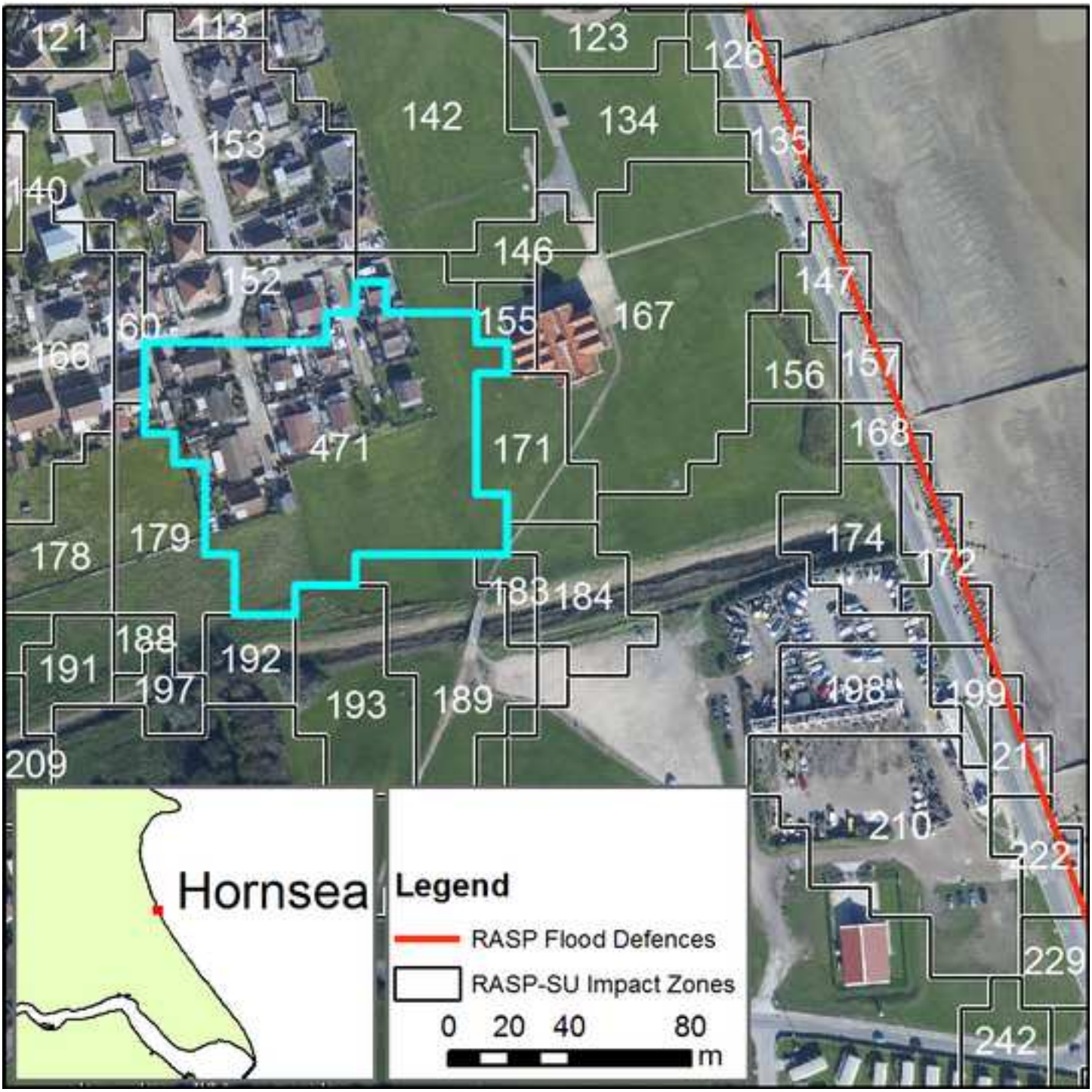

Figure 18b

Click here to download high resolution image

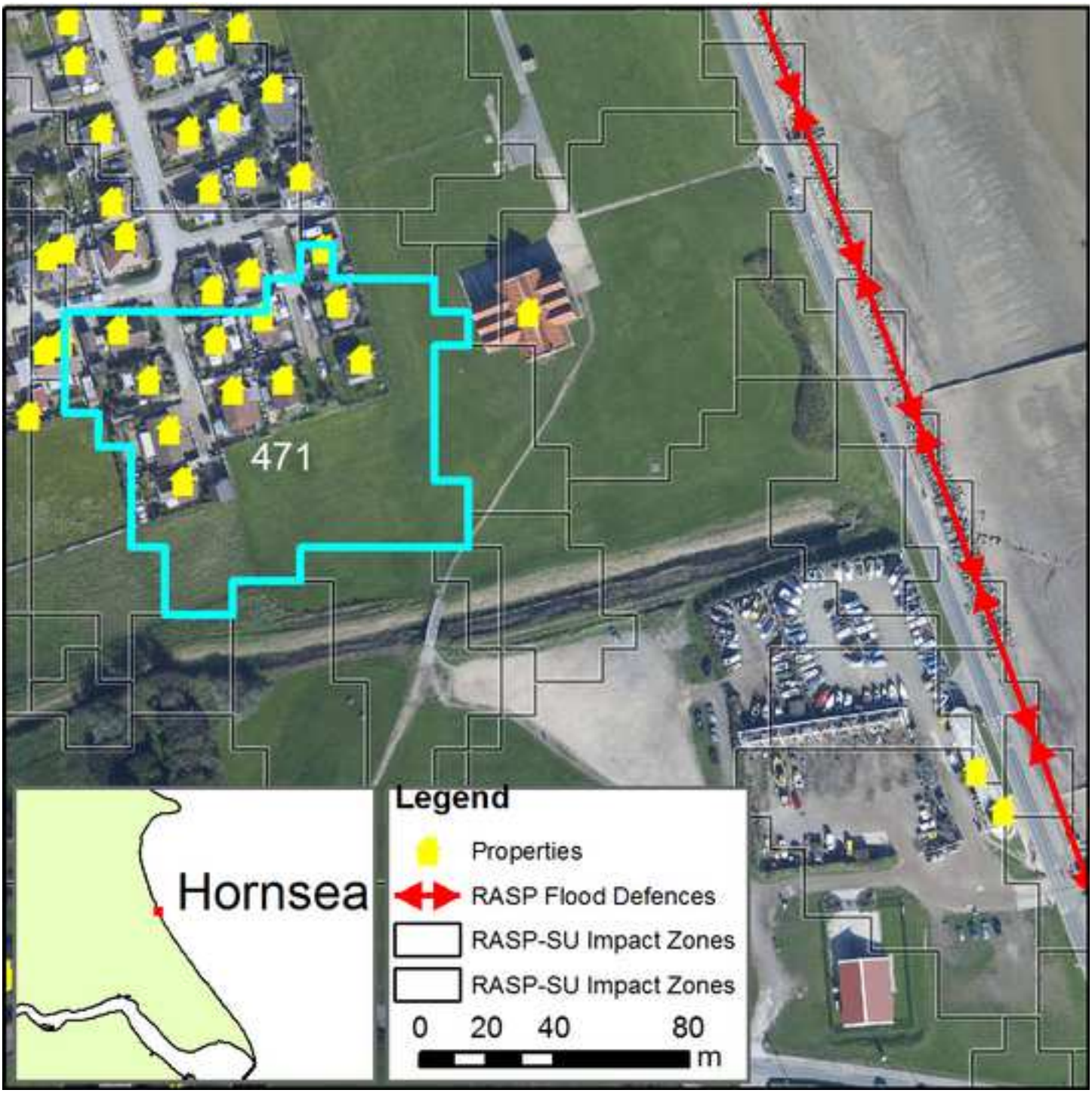

Figure 18c

Click here to download high resolution image

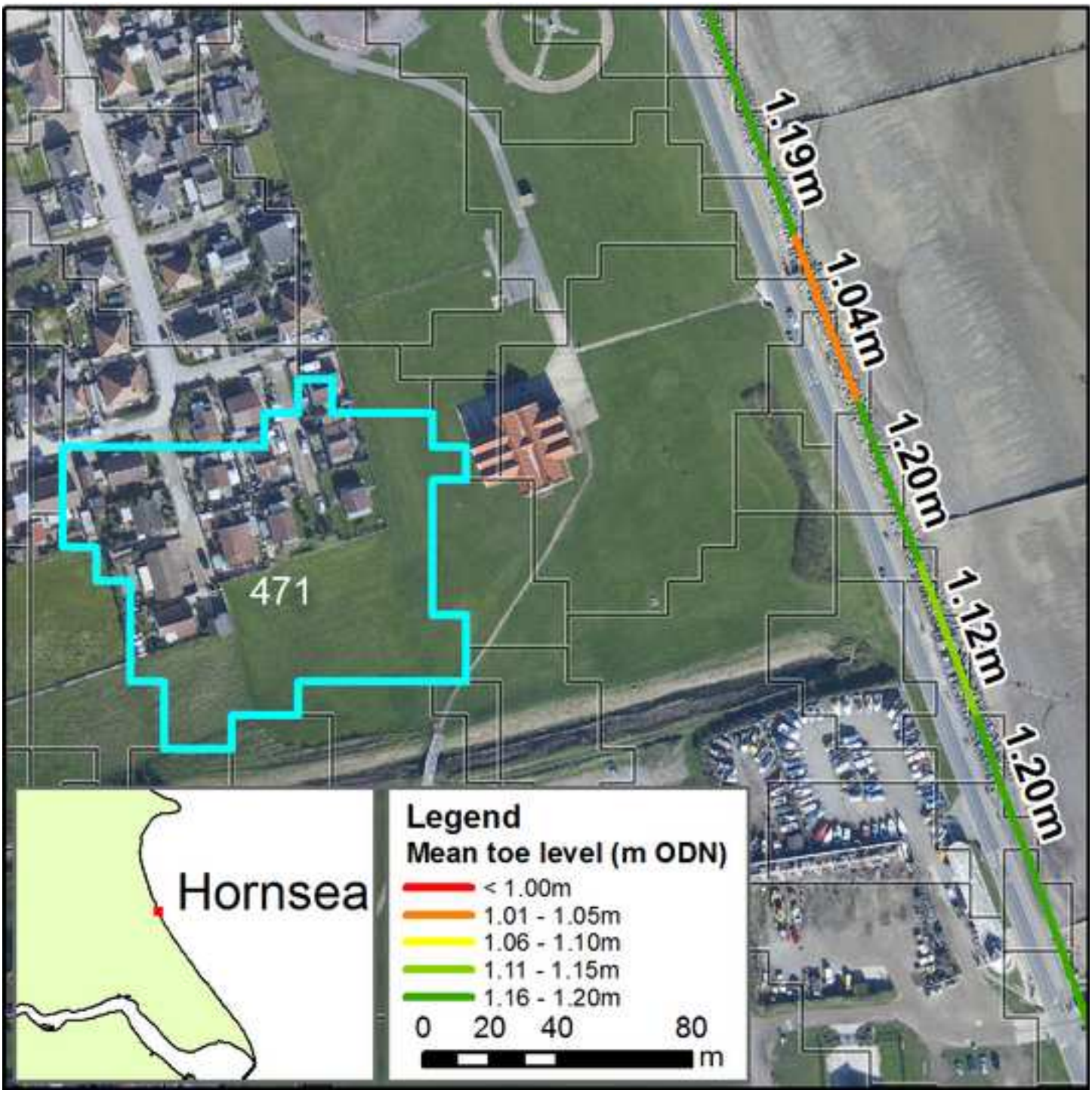

Figure 19a

Click here to download high resolution image

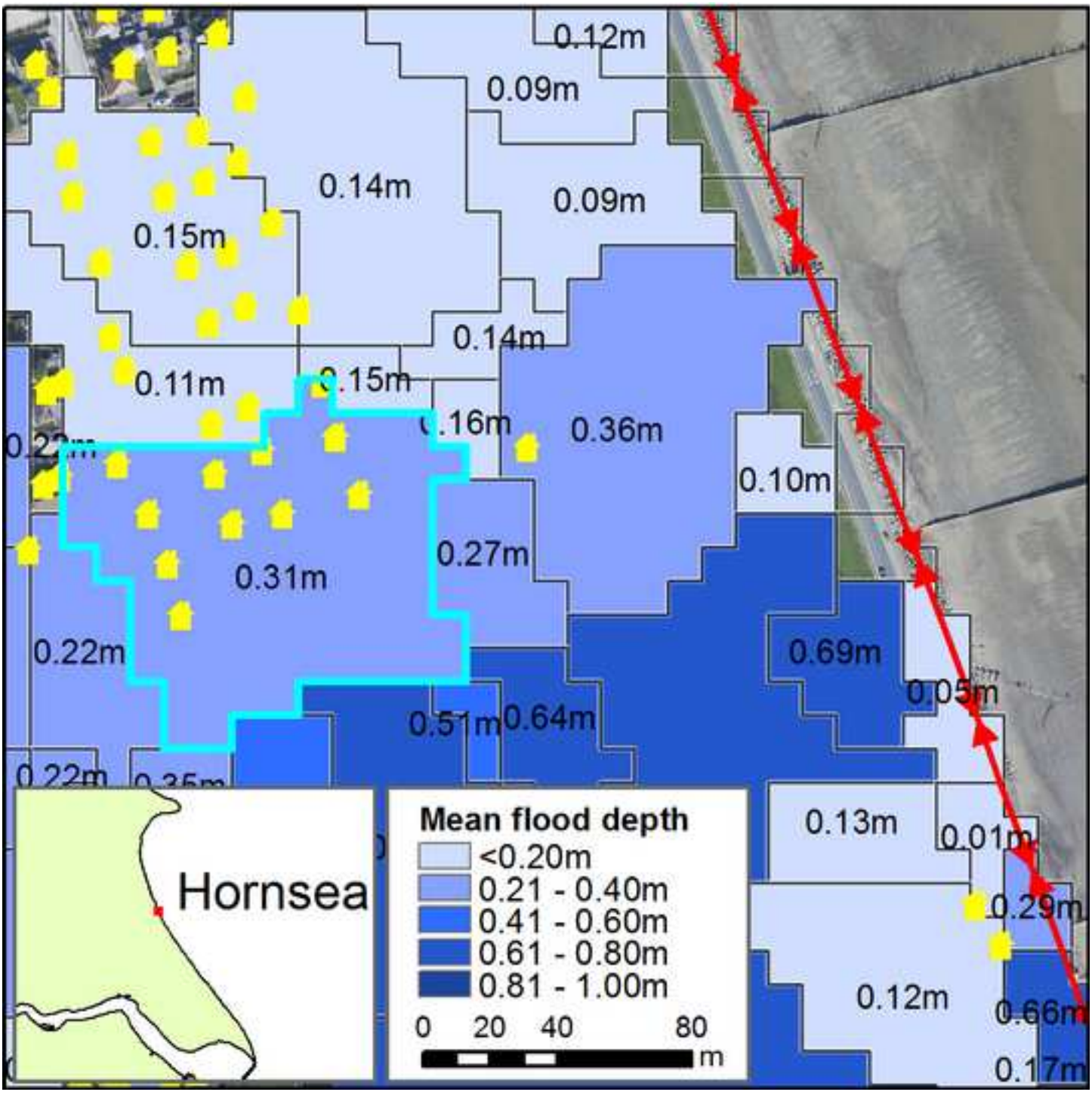

Figure 19b

Click here to download high resolution image

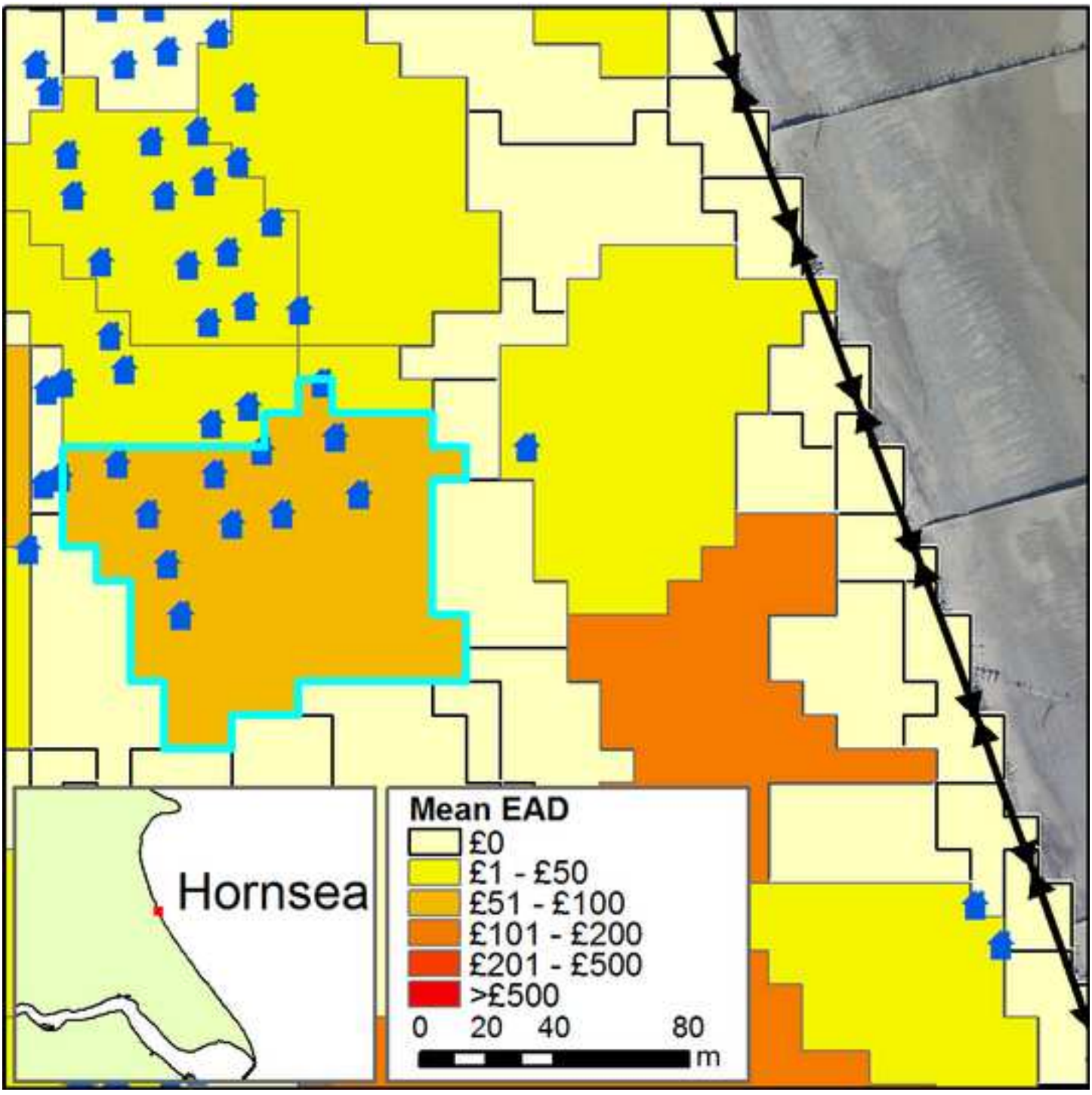

Plate List

Plate 1

Click here to download high resolution image

Plate 2

Click here to download high resolution image

Table 1

AS 1 - Infinite groyne analytical solution

dt	dx						
	75m	100m	150m	200m	250m	300m	400m
day	√	√	√	√	√	√	√
week				√	√	√	√
fortnight				√	√	√	√
month				√	√	√	√

UNSTABLE

AS 2 - Constant discharge from a source at a point

dt	dx					
	75m	100m	150m	200m	250m	300m
day	√	√	√	√	√	√
week				√	√	√
fortnight					√	√
month						√

UNSTABLE

Table 1 Comparison of range of stability for varying time and space discretisation – groyne v point source with explicit numerical scheme utilized